Available online at www.sciencedirect.com
SCIENCE DIRECT
Coordination Chemistry Reviews 249 (2005) 2489–2509
COORDINATION CHEMISTRY REVIEWS
www.elsevier.com/locate/ccr

Review

Photophysics and structure of selected lanthanide compounds☆

P. Gawryszewska, J. Sokolnicki, J. Legendziewicz*

Faculty of Chemistry, Wrocław University, 14 F. Joliot-Curie, PL-50-383Wrocław, Poland

Received 23 February 2005; accepted 24 June 2005
Available online 19 September 2005

Contents

Abstract

This paper is devoted to photophysical studies of selected lanthanide compounds defining their applicability. The photophysical behaviour of three classes of compounds will be discussed: (1) lanthanide complexes with amino acids, their phosphonic analogues and peptides, (2) lanthanide chelates as efficient luminophores, and (3) new kinds of compound applicable in biomedical assays. The majority of the results reported to date have been obtained for solutions, applying lanthanide ions as a spectroscopic probes in biologically active systems. Thus, our effort is addressed to solid-state spectroscopic and structural investigations. On the other hand advances in the development of efficient luminophores based on molecular light conversion in lanthanide chelates are presented—mainly the results of our group. Attention has been focused on: the radiative and non-radiative processes, the mechanism of the intramolecular energy transfer, the role of the charge–transfer states in this process, the electron–phonon coupling, including the resonance effect, the multi-ion cooperative interactions, and dynamics of the excited states in chiral systems—the phenomena affecting the luminescenscence efficiency. High resolution electron spectroscopy at low temperatures has been particularly useful in determining metal ion symmetry and the number of the sites.

Keywords: Photophysics; Lanthanide chelates; Spectroscopy; Structure; Energy transfer; Amino acids; Peptides

1. Introduction

Interest in the photophysical properties of lanthanide compounds has been observed for many years because of the possibility of their application in many different fields. Recently, the range of the applications has become wider—from quantum cutting materials to fluoroimmunoassays techniques [1–9]. Most of these applications are based on the optical properties of the lanthanide compounds, mainly efficient emission in the UV to IR regions. The synthesis and development of new efficient phosphors and design of the best conditions for appropriate applications become a challenge for scientists in the field of luminescence materials. Such applications of lanthanide ions and complexes as spectroscopic structural probes in biologically important systems [10–18], in chiral recognition of biological substrates [12], in selective hydrolysis of DNA and RNA [19,20], in time-resolved microscopy [8], as scavengers of free radicals [13], as solid-state materials [4,21–23], in luminescent lighting devices [4,21,24,25], in luminescence sensors [26–28] or electroluminescent devices [4,24,25,29–31] are increasingly important. Moreover, in the last decade lanthanides were used in studies of the mechanisms of several biological processes; energy and electron transfer, perforation of cell membranes [13,32], apoptosis induction [13,34], and use in medicine, in radioimmunotherapy [33], magnetic resonance

☆ We apologize to the authors whose papers have been unintentionally omitted in this report. The X-ray data which were discussed in detail in a review by Kramer et al. [53] are not covered in this article.

* Corresponding author. Tel.: +48 71 3757300; fax: +48 71 3282348.
E-mail address: jl@wchuwr.chem.uni.wroc.pl (J. Legendziewicz).

0010-8545/$ – see front matter © 2005 Elsevier B.V. All rights reserved.
doi:10.1016/j.ccr.2005.06.021

imaging [34] and others [4,12,13,33,34]. In these applications knowledge concerning the structure and spectroscopy of well-defined single crystals of the complexes is crucially important for understanding the mechanisms of interactions, function of the complexes, transport and biological activity.

In order to gain deep insight into the factors affecting the relevant optical properties of lanthanide compounds (efficiency of emission, quantum yields, photo-, thermo- and thermodynamic stabilities and other aspects of the luminescence sensitisation—critically important for applications) we have undertaken directed studies of selected lanthanide compounds important for electroluminescence devices, biomedical assays and employing lanthanide ions as structural probes in studies of biologically related systems.

The review will be divided into three sections. In the first, the state-of-art of lanthanide ions interactions with biologically active ligands will be *briefly described* and on this platform our achievements will be presented. The second section will be devoted to highly emitting luminophores, chelates, which can find applications in electroluminescence devices and sensors. The last section contains a review of the latest theoretical and experimental results on the photophysical characteristics new class of lanthanide complexes applicable in biomedical assays.

2. Lanthanide ion interactions with amino acids, peptides and related systems

The ability of certain trivalent lanthanide ions to display luminescence renders them attractive as substitutional probe ions for studies of Ca(II) binding proteins and other biologically interesting systems because lanthanide ions are recognised as being similar to divalent alkaline earth ions. Since the calcium ions are bound in proteins by aspartate and glutamate residues, so studies of lanthanide ion interactions with amino acids and peptides is essential to understand more complicated systems [4,10,15–18,31,35,36]. The Eu(III) and Nd(III) ions are particularly useful in this regard.

The laser excitation spectra of Eu(III) ion have proven valuable in providing a variety of information, including the number of coordinated water molecules [37], estimation of the total charge on the ligand atoms in the first coordination sphere [38], point symmetry determination and the number of metal sites [18,31,35,38–42], the chirality effect in the energy transfer [18,43–46], chiroptical spectroscopy, chiral probes [26], the coordination modes of amino acids and peptides under different conditions [47,48]. The majority of the studies have been devoted to solutions. In this regard the studies of Horrocks [10,17,37], Richardson [16] Nieober [15], Brittain [43,44], Darnall and Sherry [47,48], Dickins and Parker [14,36,49], Riehl [50] and others [18,35,31] are very important and pioneering.

The first example of stereoselectivity involving lanthanide complexes was discovered by Brittain [43,44], in solutions of aspartic acid. The chirality effect in the Tb–Eu energy transfer becomes important when polynuclear complexes are formed—a static mechanism for this process was proposed. The energy could be transferred more efficiently in complexes containing racemic ligands than with chirally resolved ligands.

In our studies on monocrystals of lanthanide polynuclear complexes and dimers we have proven that the energy transfer rate (from Tb(III) to Eu(III)) is different in the racemic and the resolved systems with glutamic acid, and transfer is more effective for the L-form than DL [18,45], and is in accordance with the theoretical model developed by Strek and co-worker [46] predicting more efficient transfer in the resolved systems. A similar trend for the energy transfer has been observed from the relative intensities of the $^5D_4 \rightarrow {}^7F_3/{}^5D_0 \rightarrow {}^7F_2$ transitions in the L and DL; Tb–Eu glutamic acid monocrystals.

Recently, different aspects of chirality were investigated by Parker et al. and Riehl [14,36,49,50]. Chiroptical spectroscopic studies of the interaction of the enantiopure lanthanide (Eu,Yb) complexes with self-complementary dodecamer oligonucleotides points at the distinctive selectivity in the binding affinity. The differences were dependent upon the nature of the oligonucleotide and lanthanide, e.g. Eu versus Yb [49]. Important results were obtained by Dickins et al. [30] in structural and NMR investigations of the ternary adducts of α-amino acids and selected dipeptides with chiral diaqua–ytterbium complexes. The α-amino acids bind in a bidentate manner displacing both of the water molecules with the amine nitrogen and the carboxylate oxygen. Peptides behave in an analogous manner.

X-ray analyses have evidently proven the coordination of Ln(III) ions by N and (carboxyl) oxygen atoms of amino acids. However, these unexpected results were obtained in unique conditions, e.g. for a Ln(III) chelate with almost saturated coordination by a strong chelate ligand, with significant steric hindrance and with almost no possibility to create bonding by two metal ions with the same amino acids or peptide molecules [30].

In an attempt to describe the factors affecting the structure of the lanthanide complexes with amino acids, their phosphonic analogues and peptides, in the solid state, we have used X-ray diffraction and various spectroscopic techniques in a wide range of temperatures from 4 to 300 K, with special emphasis on the detection of the chirality influence on structure, and types and dimensionality of polymers and dimers. To our knowledge the photophysics of these single crystals are the only reported data. The intensity analysis of the f–f transitions based on the static model of the Judd theory [51] and the Richardson [52] dynamic model and splitting of the levels can be related to the symmetry of the metal centre and the character of the bonding in the complexes. The cooperative interaction between the metal ions in the polynuclear polymeric and dimeric systems manifest in the single crystal spectra and the electron–phonon coupling in the electronic transitions obeying the selection rules $|\Delta J| = 2$, including resonance effects, have been investigated in high resolution absorption, emission and excitation spectra. These spectroscopic phenomena can be directly related to their structure.

The recent review by Kremer et al. [53] reports the available structures of lanthanide complexes including our results (see Table 1 of [53]). The authors characterised Ln(III) complexes with amino acids and peptides including mixed ligands and heteronuclear compounds, investigated mainly by

Table 1
Selected crystallographic data for lanthanide complexes with amino acids

Formula	Site no.	Space group	CN	Form of polymer	References
1. $[Eu_2(L\text{-}\alpha\text{-}Ala)_4\cdot(H_2O)_8](ClO_4)_6$ Nd, Eu, Ho isomorphic	2	$P1$	8	Dimer	[18,31,39]
2. $[Eu_2(DL\text{-}\alpha\text{-}Ala)_4\cdot(H_2O)_8](ClO_4)_6$ Nd, Eu, Ho isomorphic	1	$C2/c$	8	Dimer	[18,31,39]
3. $[Ln_2(L\text{-}Glu)_2\cdot(H_2O)_8](ClO_4)_4\cdot H_2O$ Ln = Ho, Dy isomorphic with Eu, Nd	4	$P2_1$	9	Polymer	[18,31,62,63]
4. $[Ln_2(DL\text{-}Glu)_2\cdot(H_2O)_8](ClO_4)_4\cdot H_2O$ Ln = Ho, Dy isomorphic with Eu, Nd	2	$P2_1/c$	9	Polymer	[18,31,62,63]
5. $[Ln(L\text{-}Ile)_2\cdot(H_2O)_4]_2(ClO_4)_6$ Ln = Pr, Nd, Eu	2	$C\bar{2}$	8	Dimer	[31,41,42]
6. $[Ln(DL\text{-}Ile)_2\cdot(H_2O)_4]_2(ClO_4)_6$ Ln = Pr, Nd, Eu	1	$P\bar{1}$	8	Dimer	[31,41,42]
7. $[Eu(L\text{-}\alpha\text{-}C_3H_8N_2O_2)\cdot(H_2O)_6]_2(ClO_4)_6$	2	$P2_1/n$	9	Dimer	[31,70,71]
8. $[Eu(DL\text{-}\alpha\text{-}C_3H_8N_2O_2)\cdot(H_2O)_6]_2(ClO_4)_6$	1	$P1$	9	Dimer	[31,70,71]
9. $[Eu_2(L\text{-}proH)_4(H_2O)_8](ClO_4)_6\cdot H_2O$	2	$P42_12$	8	Dimer	[56]
10. $[Eu(L\text{-}proH)_3(H_2O)_3](ClO_4)_3$	2	$P1$	8	Polymer	[56]
11. $Nd(Gly\text{-}Gly)_2(ClO_4)_3\cdot 4H_2O$ isomorphic with Eu	1	$P2_1$	9	Polymer	[18,40,61]
12. $Eu_2(HO_3PCH_2NH_2CH_2COO)_2\cdot(H_2O)_8(ClO_4)_4$	2	$P2_1/c$	8, 9	Two-dimensional polymer	[31,69]
13. $\{Lu(PO_3HCH_2CH_2NH_3)_3(ClO_4)_3\cdot 3D_2O\}_n$	1	$P2_1/a$	6	Polymer	[72]

Zheng and Staples [54,55]. The review collected available stability constants, thermodynamic and equilibrium data. Thus, Table 1 of our paper displays X-ray data only for compounds with unusual structures for which spectroscopic studies of the monocrystals yielded discoveries of unexpected spectroscopic phenomena.

Generally, from the five different coordination modes of carboxyl groups known, only three types have been found in complexes of lanthanides with amino acids:

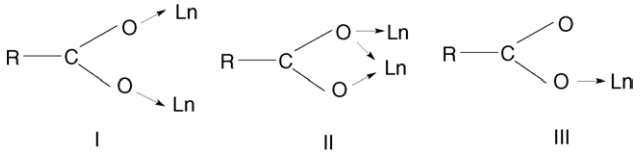

The last type is very rarely represented in lanthanide carboxylates, but has been observed in Ln(III) complexes with proline [18,56–58]. The spectroscopic data usually confirm the lanthanide ion point symmetry as determined by X-ray analyses (Table 1), although the dynamics of the solids can lead to transformation of the structures at low temperatures [35,56,59]. The single crystal spectra of the europium complex with DL-alaninehydroxamic acids (see Fig. 1) reveal that at 293 K this structure has one metal site, and at 80 K it transforms to a structure with two different metal sites.

The composition of the complexes (Ln/L ratio) may influence the mode of polymer formation in the two types of the complexes with proline: $[Ln(L\text{-}proH)_2(H_2O)_5]Cl_3$ (a) and $[Nd(L\text{-}proH)_3(H_2O)_2](ClO_4)_3$ (b) [18,56–58], Fig. 2 demonstrates these kinds of the polymers. A similar effect has been observed for the structure of monocrystals with L-α-alanine where dimers and linear polymers are formed for the 1:2 and 1:1-Ln/L ratios, respectively [59,60].

The changes in the ionic radii of the lanthanide ions can influence the structure of complexes. Eu(III), near the middle of the lanthanide series, simultaneously forms (under the same conditions) two complexes with M/L-proline ratios of 1:3 **I** and 1:2 **II** [56]. The first-with unexpectedly high tetragonal crystallographic symmetry (previously unknown for the lanthanide amino acids systems – see Fig. 1 in [56]) and the second – with the triclinic structure as observed for many other lanthanide systems (see Fig. 2 in [56]) [56–61].

Full spectroscopic characteristics have been obtained for these two kinds of compound, based on the absorption, emission and emission excitation spectra at 300 and 4 K. The differences in the structures are manifest in the splitting of the levels (Figs. 3–5 in [56]. The intensity analysis of the f–f transitions confirms the lower symmetry of the Eu(III) ion in the crystal **II.** The $^7F_0 \rightarrow {}^5D_2$ transition intensities are: $P = 4.9$ **I** and 8.4 **II** [56]. A similar relationshipship has also been observed for the relative intensities of the $^5D_0 \rightarrow {}^7F_2/{}^5D_0 \rightarrow {}^7F_1$ transitions (R) in the emission. The estimated R values for the compounds **I** and **II** are 1.79 and 2.14, respectively. Furthermore, a phase transition in the range of 70–4 K has been detected for the crystal **I**, from analysis of the intensity changes with temperature and splitting of the ^7F_J levels.

In fact, the changes of complex stoichiometry not only influence the mode of polymer formation in the crystal structure but also the coordination mode of the carboxyl group (see Fig. 2a and b). The change of the ionic radius affects the coordination of the lanthanide ions as already described for the Ln(III) complexes with proline. In the structure of the larger Pr(III) ion complexes with glutamic and aspartic acids the perchlorate ions are involved in coordination [18,31,62–64].

The first type of coordination of the carboxyl group usually forces CN = 8, but combination of coordination types I and II usually leads to CN = 9.

Another factor, which affects the structure of the complexes is the number of carboxyl groups in the amino acids. Fig. 3 shows the structure of the $[Ho_2(L\text{-}Glu)_2(H_2O)_8](ClO_4)_4\cdot H_2O$ crystal where different coordination modes of the α and γ carboxyl groups of the glutamic acid molecules are clearly demonstrated [35,65]. A quite different structure occurs for $[Ho(Asp)(H_2O)_5]Cl_2\cdot H_2O$, although the differences in the α and β carboxyl groups bonding mode are still present. In fact, here the α-carboxylate acts as a monodentate and allows the formation of infinite chains, see Figs. 1 and 3 and Table 2 in [64].

The chirality of the amino acids influences the structures of the complexes and further the energy transfer Tb(III) → Eu(III).

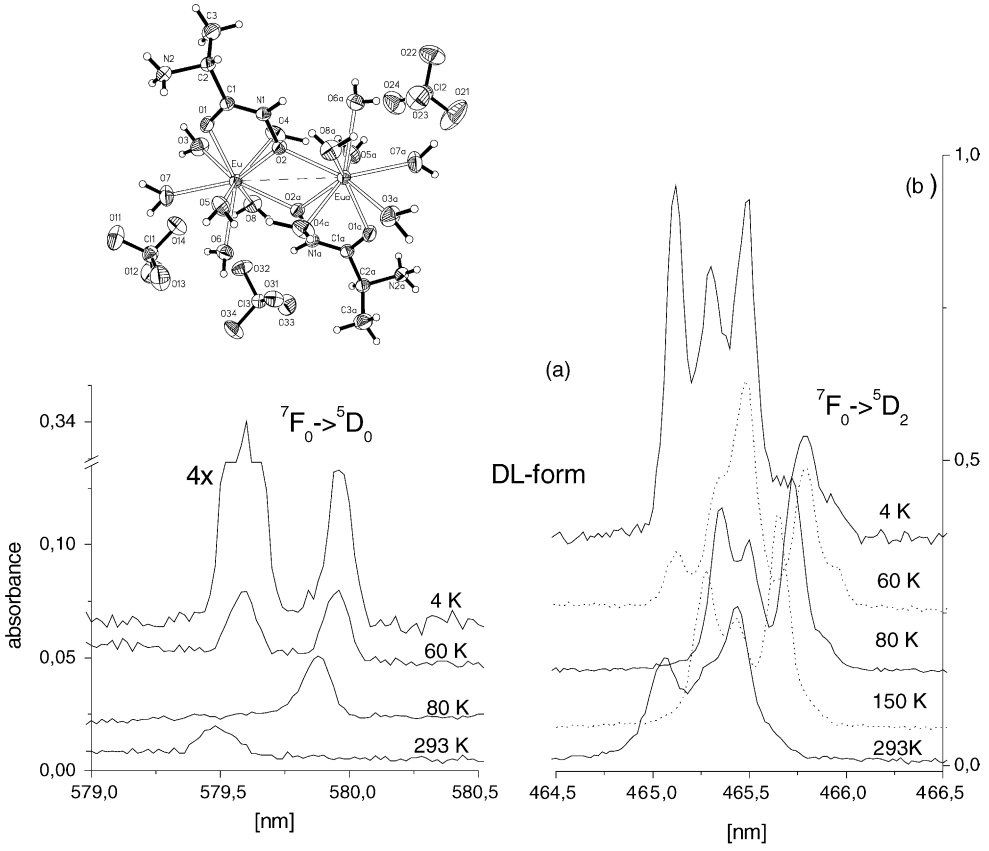

Fig. 1. (a) Crystal structure of the $[Eu(DL\text{-}\alpha\text{-}Alaha)\cdot(H_2O)_6]_2\ (ClO_4)_6$; space group $P2_1/n$; the non-centrosymmetric dimer is formed in the complex with L-α-alanine-hydroxamic acid [35,69]. (b) Temperature dependence of the $^7F_0 \rightarrow {}^5D_0$ and $^7F_0 \rightarrow {}^5D_2$ transitions in the spectra of $[Eu(DL\text{-}\alpha\text{-}Alaha)(H_2O)_6]_2(ClO_4)_6$ crystal, The structural transformation between 80 K → 60 K → 4 K. Adapted from [31,70].

This phenomenon was discovered in the L- and DL-amino and aminohydroxamic acids complexes [39,41,42,45].

Table 1 displays the X-ray data for eight complexes as do Table 4 in [18] and Table 1 in [31]. The X-ray analysis shows, for the first time, the chiral effect in the crystal structures, reflected by the symmetry of the dimer units and bonds lengths [18,31,39,41,42,66–69]. The replacement of the L form of an amino acid by the DL one converts the noncentrosymmetric dimer unit of the 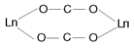 or 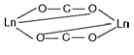 type to the centrosymmetric one of the same kind. In other words, in the former case, the two lanthanide ions in the dimeric unit are nonequivalent, but in the latter case they are equivalent and behave as a single site (Figs. 4 and 5 and 1–8 in Table 1) [18,39,41,42,68]. Consequently, through this transformation the effective number of sites is reduced by a factor of two. This effect is well reflected in the spectroscopic data.

The absorption spectra of the neodymium single crystal with L and DL alanine at 5 K and europium luminescence spectra are plotted in Figs. 5a and b, and 6a and b. The splitting of the $^{2S+1}L_J$ levels excellently detects two equivalent and two nonequivalent metal sites in the dimer units. The number of the sites is clearly shown mainly in the $^4I_{9/2} \rightarrow {}^2P_{1/2}$; $^4F_{3/2}$ transitions, the one site in the spectrum (b) and the two sites in spectrum (a) (Fig. 5). Absorption and luminescence spectroscopy at low temperature are the only methods sensitive enough to detect such subtle structural changes. Broadening of the lines can be caused by double excitation in the centrosymmetric dimer (Fig. 5b). The double excitation could go as follows: at 5 K the electronic excitation $^4I_{9/2} \rightarrow {}^{2S+1}L_J$ of one Nd(III) ion is coupled to the $^4I_{9/2}(0) \rightarrow {}^4I_{9/2}\,(i)$ (i = 1–5) of the second Nd(III) ion in the dimer [35,39]. The same mechanism of cooperative transitions takes place in the single crystal spectra of $[Ln_2\ (Ile)_4\ (H_2O)_8]\ (ClO_4)_6$ (where Ln = Pr, Nd) complexes with iso-leucine [35,41,42]). The carboxylic bridges offer efficient molecular pathways for the exchange interactions and are active for the double excitations. The cooperative interactions usually occur in polymeric and dimeric structures.

The effect of chirality has also been observed for the absorption and luminescence single crystal spectra of the L and DL-glutamic acid complexes [18].

There are four sites of Nd(III) in the structure of the complex with the L-handed acid, so four components of the $^4I_{9/2} \rightarrow {}^2P_{1/2}$ transition and two bands (each split into four components) of the $^2F_{3/2}$ state are observed at 5 K (see Fig. 7).

In the racemic crystal a reduction of the number of metal sites has been observed (see Fig. 6 [35]).

Applying the Judd theory for intensity calculations of the f–f transitions, carried out for the first time for the three orientations of the crystals, in the spectra of the neodymium and holmium

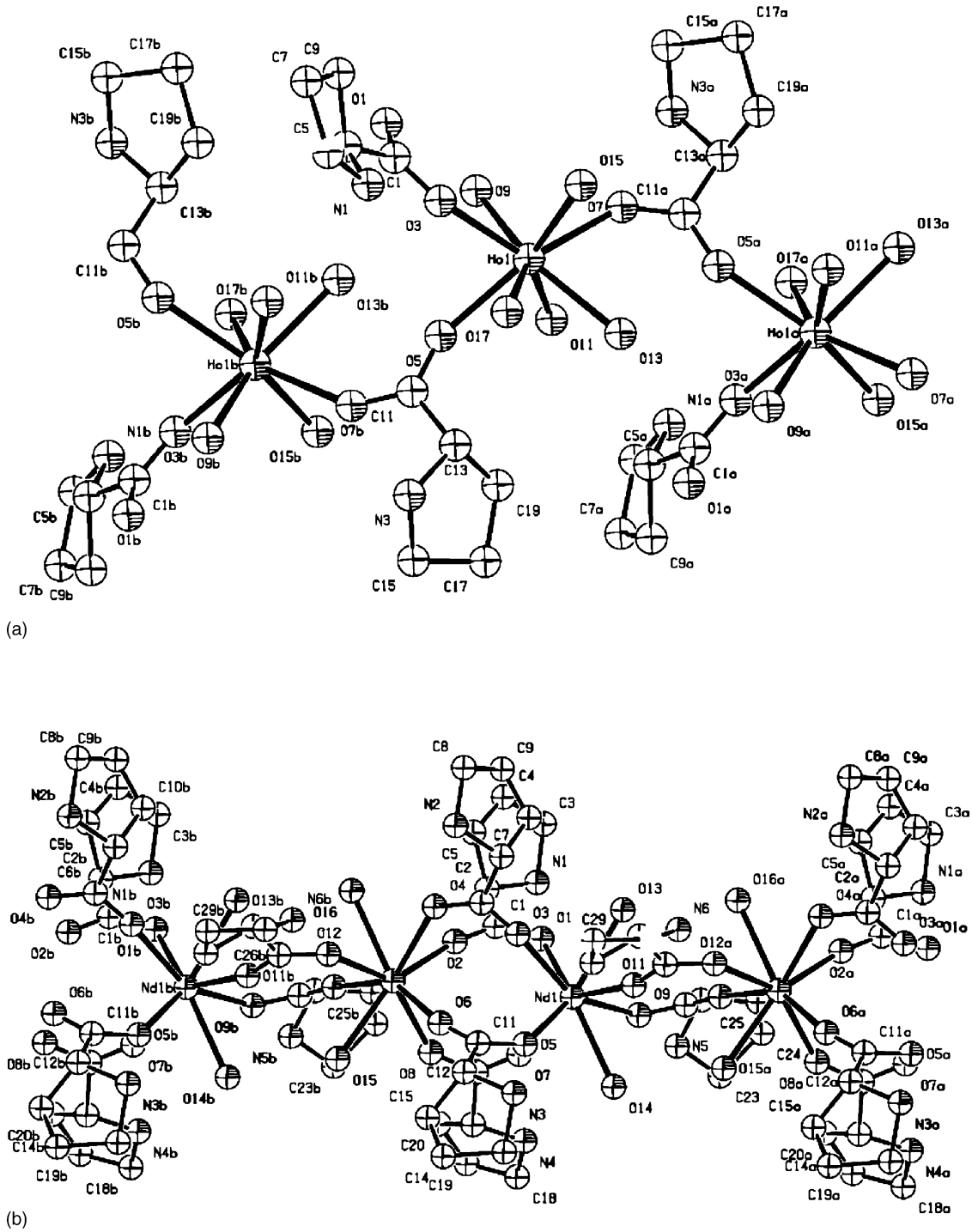

Fig. 2. (a) and (b) Different ways of the polymers formation in the structures of $[Ho(L\text{-}proH)_2(H_2O)_5]Cl_3$ and $[Nd(L\text{-}proH)_3(H_2O)_2](ClO_4)_3$ monocrystals, adapted from (a) [18,57] and (b) [18,56,58].

complexes with glycine, alanine and glutamic acid, revealed the intensity increase for the system with glutamic acid—see tables in [66,67]. This may be due to a contribution of covalency since the symmetry of the metal ions (C_{2v}) was the same in all the compounds [39,41,63,66,67,73].

In the neodymium crystals the emission is mainly quenched by the cross-relaxation whereas the multiphonon relaxation is less efficient [18,35,40].

The non-radiative luminescence quenching of the Dy(III) emission in the aminoacid systems [60] and the Pr(III) as well as Eu(III) emission quenching by Cu(II) ion in a simple carboxylate [74] have been examined. This phenomenon observed in heteronuclear systems can be crucially important for determination of the metal sites in the copper binding proteins. Using the Eu(III) ion as a spectroscopic probe, its emission can be quenched by Cu(II) if located close enough to the Eu(III) ion;

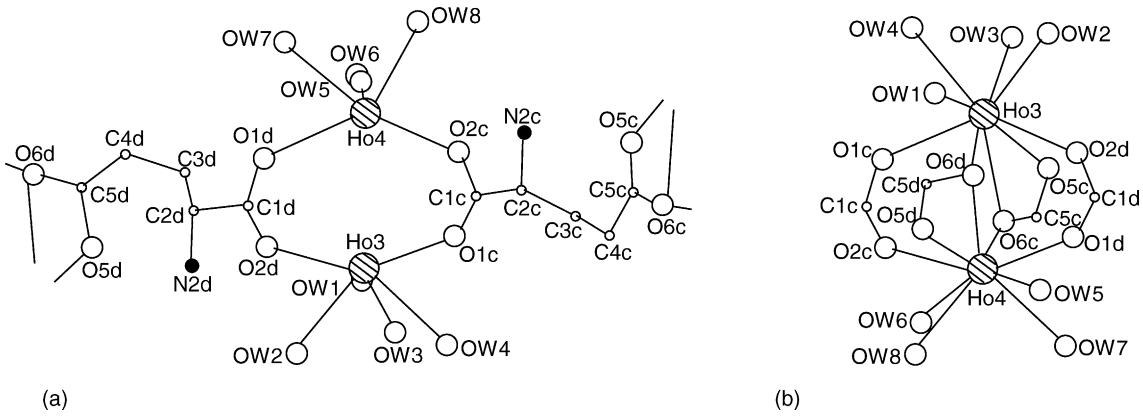

Fig. 3. Coordination of the crystalographically independent pair of the $[Ho_2(L\text{-}Glu)_2\cdot(H_2O)_8](ClO_4)_4\cdot H_2O$ crystal, adapted from (b) [18,63]. (a) The two different coordination modes of the α and γ carboxyl groups of the L-glutamic acid.

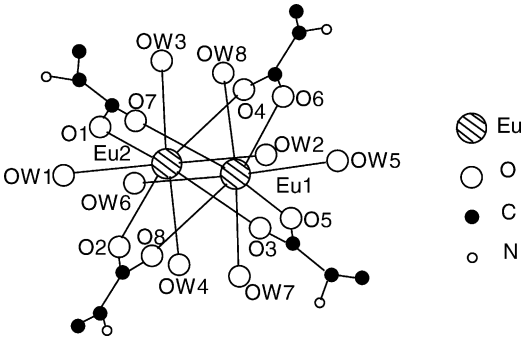

Fig. 4. Perspective view of the coordination around the pair of trivalent europium ions; in non-centrosymmetric dimer formed in the lattice of the $[Eu_2(L\text{-}\alpha\text{-}Ala)_4\cdot(H_2O)_8]\,(ClO_4)_6$ crystal, adapted from [18,39].

the loss of signal provides useful information about the location of metal sites in the protein. Moreover, this can be applied in studies of the photophysical behaviour of the green and yellow fluorescent proteins and the processes in which they are involved in [75].

More complex chains are formed in compounds with phosphonic analoques of amino acids [69,71]. Fig. 8 presents the architecture of the two-dimensional polymeric structure of the europium complex with phosphono-methylglycine (EuPMG) in which the oxygen atoms of the perchlorate anions are engaged in metal ion coordination in addition to the PMG groups. The two types of centrosymmetric dimeric units are formed by the carboxyl and phosphonic groups.

The electronic spectra also confirm the complex structure. The $^5D_0 \rightarrow {}^7F_0$ transition shows two metal ion sites, and the shift of the $^5D_0 \rightarrow {}^7F_0$ emission lines can be treated as the nephelauxetic effect caused by carboxyl and phosphonic group coordination. Vibronic components in the transitions obeying the selection rule $|\Delta J| = 2$ were observed and assigned. The modes, which promote the vibronic transitions are mainly associated with those groups which are coordinated to the metal ion [35,60,69]. This fact is important for studies of metal ion bonding in biological systems. The results are in good agreement with the theory of vibronic transition probabilities, discussed by Blasse et al. and described as follows [76]:

$$P_\nu = \nu(g + n\alpha R^{-3})^2 \Xi^2_{(1,2)} \langle J \| U^{(2)} \| J' \rangle^2 [1/(2J+1)] \times \langle 0 \| T^{(1)} \| p \rangle^2 \quad (1)$$

where P_ν is the oscillator strength of the vibronic transition involved at frequency ν, n the number of the ligands around the metal ion (M), g and α are, respectively, the charge and the polarizability of the ligand and R is the M-ligand distance. The factor $\Xi_{(1,2)}$ has been defined by Judd [51], and is related to the opposite-parity configuration mixing; and J and J' are quantum numbers for the initial and final electronic states. $\langle \| U^{(2)} \| \rangle$ is the matrix element of the reduced tensor operator, and $\langle \| T^{(1)} \| \rangle$ is the matrix element of the operator connecting the (0) and (p) vibrational states.

The last terms in this relationship remains the same for the system under consideration. Thus, the intensities of the vibronic

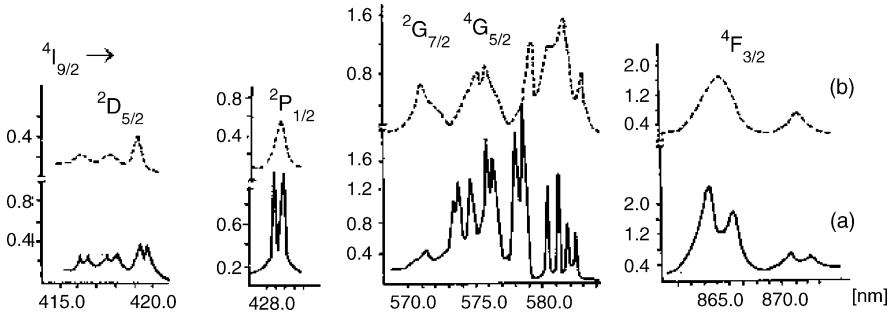

Fig. 5. Absorption spectra of the $[Nd_2(L\text{-}\alpha\text{-}Ala)_4\cdot(H_2O)_8]_2\,(ClO_4)_6$ (a) and $[Nd_2(DL\text{-}\alpha\text{-}Ala)_4\cdot(H_2O)_8]_2\,(ClO_4)_6$ (b) crystals at 5 K. Dublet structure of the band in the spectrum (a) point at two nonequivalent metal sites in the dimer, adapted from [31,39].

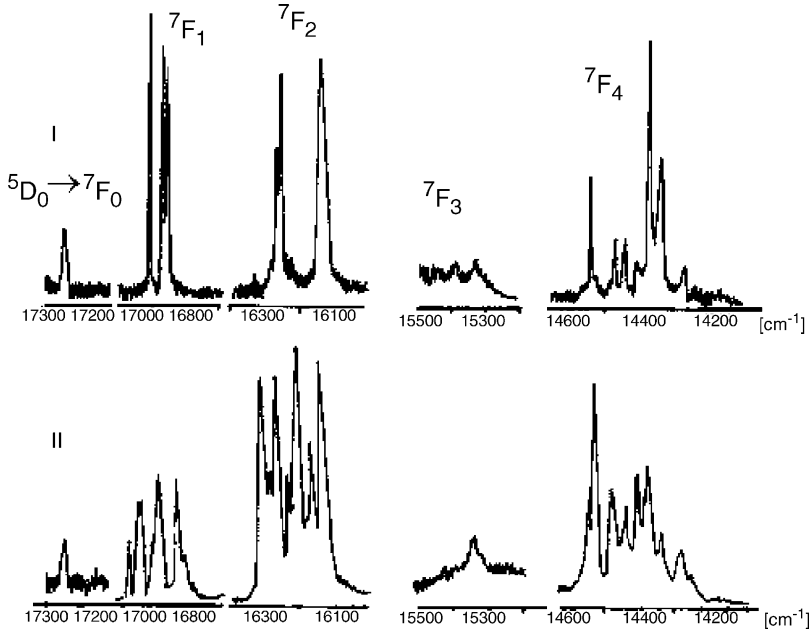

Fig. 6. Luminescence spectra of the $Eu_2(Glu)_2(ClO_4)_4{\cdot}9H2O$ at 5 K (I – DL-Glu, II – L-Glu), adapted from [31].

components correspond to the strength of the metal-ligand bonding and the ligand charge and polarizability.

Fig. 9a displays the chain built of the centrosymmetric dimers in the structure of the $Nd(Gly\text{-}Gly)_2(ClO_4)_3{\cdot}4H_2O$ crystal [18,61]. The Nd(III) ion is nine-fold oxygen coordinated. Both carboxyl and carbonyl groups of glycylglycine (I) are involved in the metal ion coordination, thus forming the chelate rings, which stabilize the crystal structure. There are two types of glycylglycine molecules in the structure. The second one binds the lanthanide ions by a simple carboxyl bridge, while the carbonyl group links other lanthanide ions. The type of lanthanide coordination in the dipeptide is the same as for glycine [31,67].

The linear polymer in the second dipeptide; Ho (Gly-L-Tyr)$Cl_3{\cdot}6H_2O$ lattice is arranged in the same manner as in the $[NdCl_3(H_2O)_3$ (β-AlaH)] crystal (b) forced by chloride ions [68]. The carboxyl bridges of type I link the metal ions and tyrosine rings are placed on one side of the polymeric chain as shown in Fig. 9b [77]. Only one site of the metal ion exists in the structure. In the holmium peptide coordination of the metal is not the same as in the glycine complex. Thus, it is not a simple rule (as we have expected) that the coordination of particular amino acid residues of the peptide will be the same as in the amino acids complexes [18,31,61,67,77].

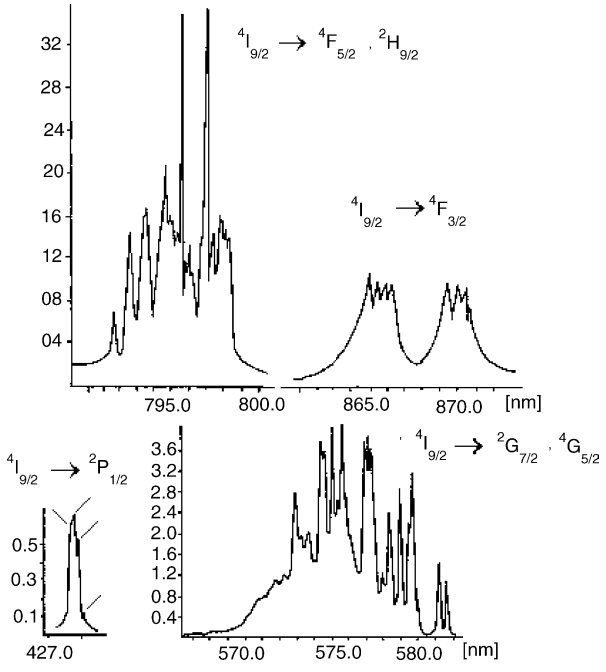

Fig. 7. Absorption spectrum of the $[Nd_2(L\text{-}Glu)_2{\cdot}(H_2O)_8]$ $(ClO_4)_4{\cdot}H_2O$ at 5 K. Splitting of the $^4F_{3/2}$ and $^2P_{1/2}$ states indicate for four metal sites in noncentrosymmetric dimeric units in the polymer, adapted from [31].

The laser-excited luminescence spectra of the Eu(III) monocrystals with glycyl-glycine correlate well with the X-ray data. The symmetry of the metal ion was established from the high resolution spectra at 77 K, as shown below in Fig. 10 [18,77].

Investigation of the absorption spectra at 300 and 4 K allows detection of the number of sites (based on $^2P_{1/2}$ Kramers doublet state of Nd(III)) see Figs. 5 and 7. These results find confirmation in the laser selectively excited luminescence spectra of Nd(III) and Eu(III). The symmetry of the Ln(III) ions was determined as shown in the spectrum in Fig. 10 [18,39–42,56,58,61]. From the low temperature luminescence spectra and absorption spectra the energy levels diagram for the ground and first excited states of Nd(III) ion could be proposed (Fig. 11).

The luminescence spectra of the monocrystals listed in Table 1 and those of other complexes have been published [18,31,35,39–42,56,68,69].

The isomorphous replacement of the Ca(II) and/or Mg(II) ions by Ln(III) ions provides the promise of exploiting the

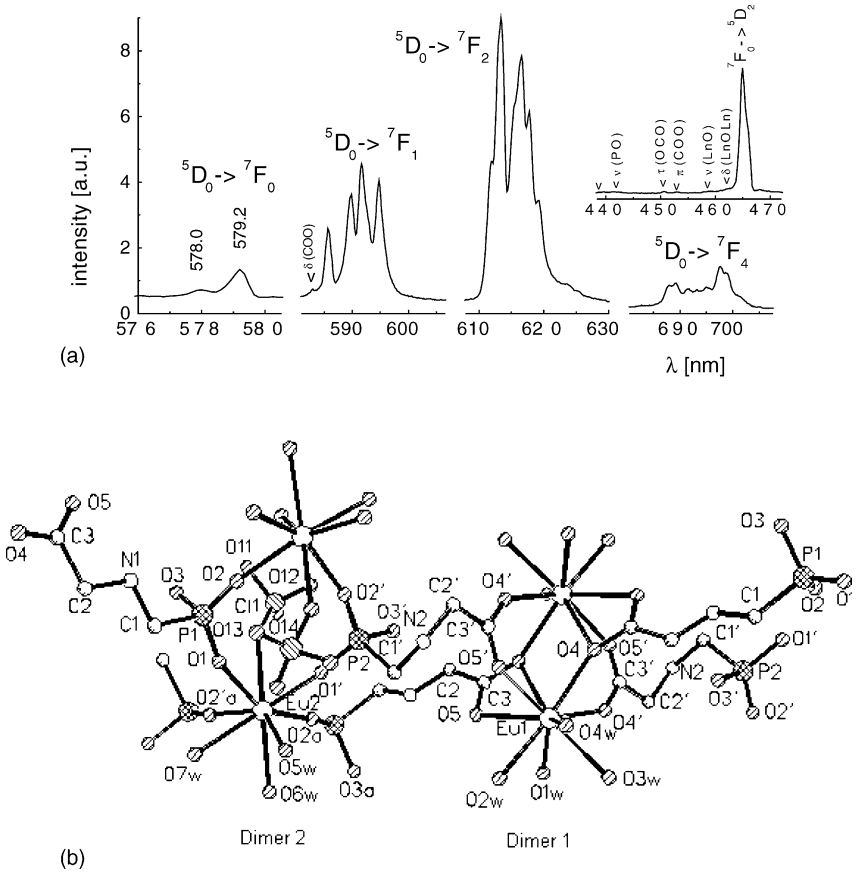

Fig. 8. (a) Emission spectra of the $Eu_2(HO_3PCH_2NH_2CH_2COO)_2(H_2O)_8(ClO_4)_4$ at 77 K, insert shows excitation spectrum of the $Eu_2(HO_3PCH_2NH_2CH_2COO)_2(H_2O)_8(ClO_4)_4$ at 77 K with vibronic components. (b) SHELXTL (XP) drawing of the $[Eu_2(HO_3PCH_2NH_2CH_2CO_2)_2(H_2O)_7(ClO_4)](ClO_4)_3\ H_2O$ structure, showing the two dimeric subunits. The polymer layer is parallel to the (1 0 2) plane.

rich and varied spectroscopic properties of the Ln(III) ions for obtaining information on the structural aspects of Ca(II) and Mg(II) biochemistry. Our detailed studies have proved different coordination of lanthanide and alkali metal by organic ligands in complexes with glycine (compare Fig. 2 in [78] and Fig. 3 in [67] for Ca(II) and Nd(III) ions, respectively), glutamic acid (Fig. 4 in [79] and Fig. 3) and peptides (Fig. 1 in [80] and Fig. 9). In the first case, the calcium atom is coordinated by seven oxygen atoms—five from the glycine molecules and two from the water molecules, forming a distorted pentagonal bipyramid. In the Nd(III) compound the carboxyl groups are bidentate and tridentate and form linear polymer chains in the structure.

The differences observed for the calcium and lanthanide structures with glutamic acid are much more significant. The calcium ions are coordinated to six oxygen atoms; five come from the carboxyl groups and one from a water molecule.

In both monocrystals with peptides, the Ca and Ln ions are bonded by the carboxyl and carbonyl groups oxygen atoms. However, the coordination number is different. Although in both compounds similar carboxyl bridges of the type (II) bind two different metal ions, addition of the two type (I) bridges strengthens the bonding between the two lanthanide ions. Such behaviour can influence the rate of the exchange of lanthanide ions in the peptide and can lead to differences in the exchange rate for the Ca(II) and Ln(III) ions. How such changes influence the function of the peptides and proteins in biological systems, is difficult to say. We have also found an isomorphic substitution of calcium by lanthanide ions in case of ciliatine (Table 1) and some dipeptides[17,77,72,81].

3. Ln(III) β-diketonates of $NaLn\beta_4$ and $Ln\beta_3L$ types

The development of efficient organic light emitting diodes (OLEDs) [82] and polymer light emitting diodes (PLEDs) [83] has lead to new possibilities for a low cost, compact display technology. However, the broad emission observed from most organic molecules (due to the vibrational broadening) makes the spectroscopic purity required for red, green, blue displays difficult to achieve. The use of rare earth ions-containing organic molecules is, however, a possible route to obtaining such emission with a theoretical upper limit of inner quantum efficiency near 100% and has renewed interest in these molecules. Using an appropriate organolanthanide complex for the emission layer one can achieve electroluminescence (EL) covering the spectrum from blue to infra-red [29,84,85]. OLEDs with molecules incorporating Eu(III) emit red [86,87], Sm(III) red-orange [88–91], Tb(III) green [87,92,93] and Tm(III) blue light [94]. OLEDs incorporating Nd(III) [95–98], Yb(III) [95,96] and Er(III) [98,99] have recently been demonstrated

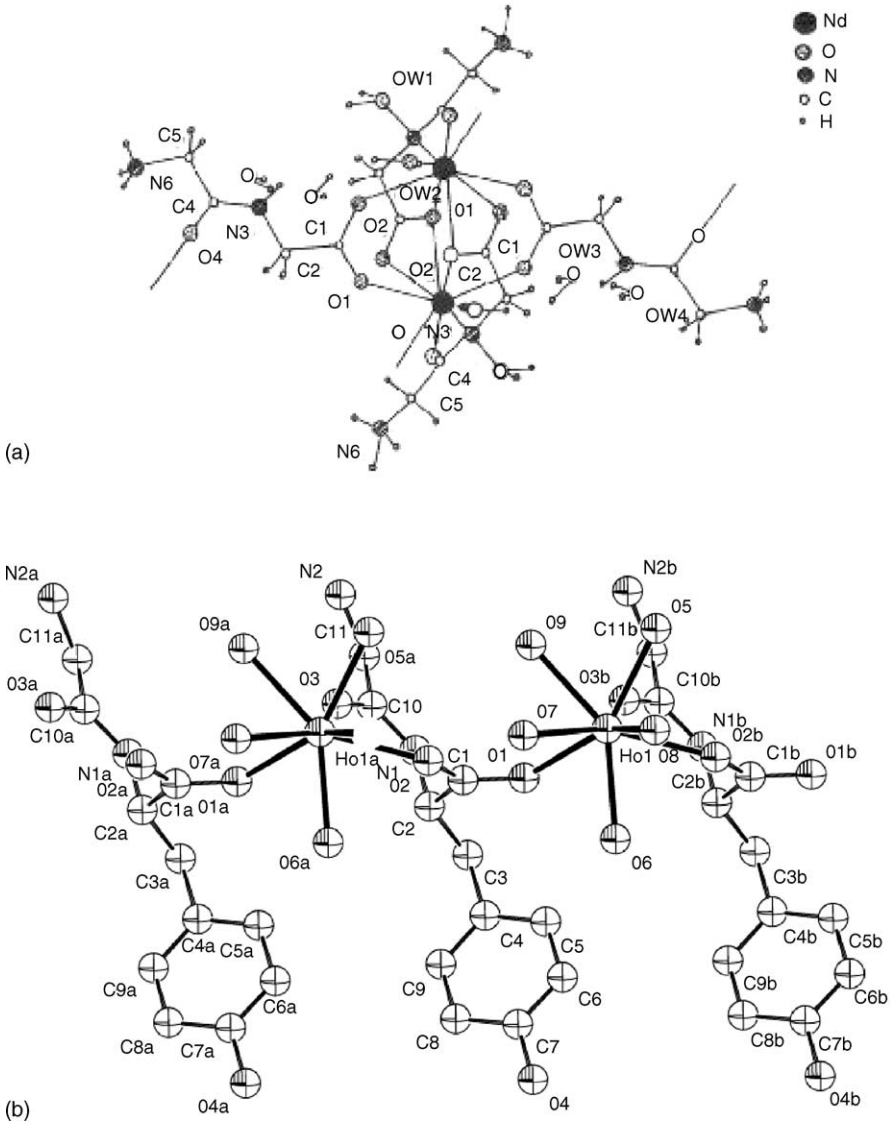

Fig. 9. View of the structure of the $Nd(Gly\text{-}Gly)_2(ClO_4)_3{\cdot}4H_2O$ crystal (a) [18,31,35,61]. One-dimensional infinite chain in the structure of the $[Ho(C_{11}H_{14}N_2O_4){\cdot}(H_2O)_5]Cl_3{\cdot}H_2O$ (b) [31,77]. Reprinted with permission from Ref. [61].*Copyright 1992 International Union of Crystallography Blackwell Munksgaard*.

to exhibit infra-red emission. Other lanthanide ions used in OLED studies include Pr(III) [100], Gd(III) [101,102] and Dy(III) [103,104]. The quantum efficiencies of these devices are lower then those reported for Eu(III) and Tb(III) devices. Factors responsible for this include non-radiative relaxation of the excited rare earth ion and poor charge injection and transport.

Since subtle changes in the molecular structures of the Eu(III) complexes could dramatically tune the photoluminescence and EL properties, the development of new Eu(III) β-diketonate mixed ligand complexes for the light-emitting layers of the EL device is a prevailing research activity [87,91,92,105–114]. The research efforts include design of new β-diketones and neutral second ligands [108,115], usually 2,2′-bipyridine, 1,10-phenanthroline and trioctylphosphine oxide [100,116,117]. This combination fills all coordination positions of the metal ion providing a stable complex. Thus, most of the published work

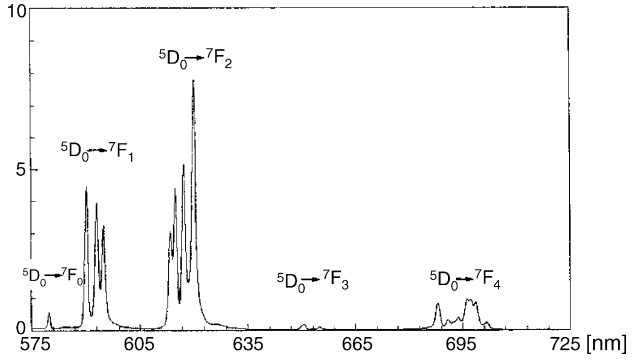

Fig. 10. Luminescence spectrum of the $Eu(Gly\text{-}Gly)_2(ClO_4)_3{\cdot}4H_2O$ crystal at 77 K, adapted from [40].

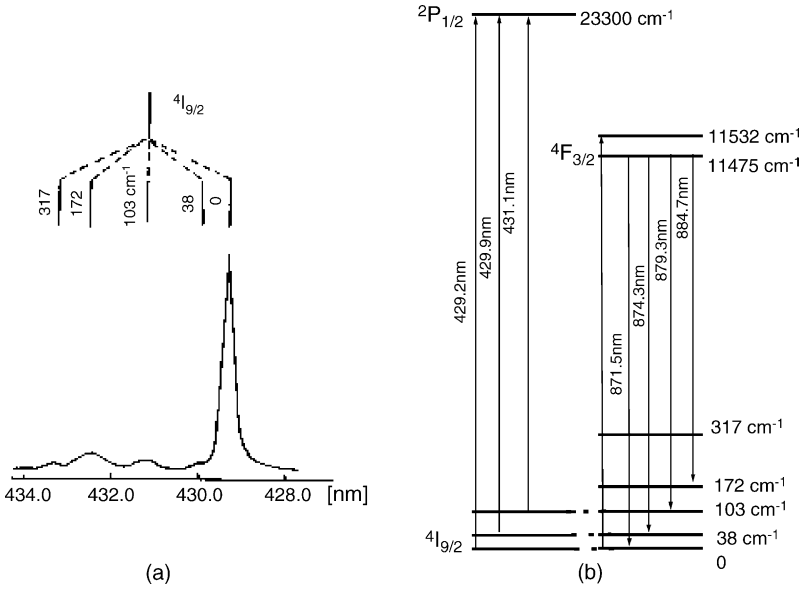

Fig. 11. (a) The $^4I_{9/2} \rightarrow {}^2P_{1/2}$ transition in absorption spectrum of the $[Nd(L\text{-}proH)_3(H_2O)_2](ClO_4)_3$ crystal at 293 K. (b) The energy level diagram of $^4I_{9/2}$ state proposed on the basis of luminescence spectrum at 77 K, adapted from [58].

covers these basic ligands and differ in the choice of their derivatives. Chemical modification of the neutral ligand or β-diketone is dictated by three major principles: (1) the complex lowest triplet level must match the metal emitting state, being, ideally—slightly, above it [118]; (2) for EL applications it is considered advantageous to enrich the ligand(s) with electron and hole-transporting chemical groups in order to facilitate charge carrier injection and exciton trapping in the complex [119]; (3) the complex must be thin-film forming upon vacuum deposition without aggregation or crystallization problems. It also must be miscible with other species (if necessary) as well as thermally stable [120].

Various spectroscopic methods as well as X-ray data have been used to investigate structural peculiarities for a variety of lanthanide compounds. Our interest has been to determine the influence of the donor–acceptor properties and of the size of the ligands on the spectroscopic characteristics of a series of lanthanide β-diketonates. In particular, these donor–acceptor properties influence the ligands and Ln(III) ions absorption and luminescence transitions energy and intensity, the vibrational states, the electron–phonon coupling as well as the energy transfer and the quantum yields of the luminescence of lanthanide β-diketonates. Analysis of the total spectroscopic data permits the evaluation of the applicability of different β-diketonates in OLEDs.

For this investigation we have chosen europium β-diketonates with 1,10-phenanthroline derivatives or 2,2′-bipyridine as a second ligand [25,30,35,121–124]. Spectroscopic data, including the nephelauxetic effect (shifts of the $^5D_0 \rightarrow {}^7F_0$ transition), the crystal field parameters and intensity ratios of the emission transitions for a series of europium β-diketonates are collected in Table 2.

Increase of acceptor properties of one ligand of the compound is equivalent to increase of the donor properties of the other lig-

Table 2
Positions of $^5D_0$ level (cm^{-1}), crystal fields parameters (cm^{-1}) and intensities of $^5D_0 \rightarrow {}^7F_2$ transition

Compound	$^5D_0 \rightarrow {}^7F_0$ 77 K	B_0^2	B_2^2	B_0^4	B_2^4	B_4^4	I_{0-2}/I_{0-1}	
		CFP, 77 K					77 K	300 K
$Eu(DPM)_3$ phen	17241	705	87	−1605	−536	733	12.1	9.2
$Eu(AA)_3$ Tmphen	17221	580	122	−1424	−466	758	8.2	9.7
$Eu(AA)_3$ Phen	17247	653	188	−1413	−530	772	7.8	7.0
$Eu(BA)_3$ Phen	17256	596	175	−1603	−594	671		
$Eu(FOD)_3$ Tmphen	17209	425	105	−1519	−578	520	12.0	
$Eu(FOD)_3$ Phen	17238	472	198	−1547	−530	590	11.9	13.2
Eu(FOD) Dphphen	17212	490	221	−1615	−531	573	12.2	
$Eu(FOD)_3$ Nphen	17209	553	139	−1571	−515	737	12.0	
$Eu(TTF\ A)_3$ Tmphen	17235	345	180	−1636	−565	537	13.9	16.3
$Eu(TTFA)_3$ Phen	17244	622	116	−1580	−629	759	10.2	11.4
$Eu(TTF\ A)_3$ Nphen	17241	635	87	−1606	−615	726	12.6	12.4
$Eu(GOFGD)_3$ Phen	17230	518	94	−1659	−678	541	12.3	13.8
$Eu(OTOFOD)_3$ Phen	17221	520	105	−1751	−579	608	11.8	13.8

and in regard to the effective charge distribution on the atoms of the local environment of the Ln(III) ions. This leads to gradual changes in the crystal field (CF) that appear as gradual changes of the Ln(III) electronic spectra represented by the nephelauxetic shift, the crystal field parameters and intensity ratios of the emission bands (see Table 2).

Substituents with different donor–acceptor properties in the β-diketone molecules change the distribution of the π-electronic density in the chelating rings as well as the effective charges on the oxygen atoms. This leads to a change in covalency of the Ln–O bond, and changes of the bond strengths and distances in the Ln–O and Ln–N cases. Similar effects are observed with variation of substituents for the other ligand (1,10-phenanthroline). The degree of covalency of the metal–ligand bonds may be characterized by shifts of the $^5D_0 \rightarrow {}^7F_0$ transition in the Eu(III) spectra. The most effective luminescence of Eu(III) is observed through ligand band excitations, where the ligand bands are in resonance with the $^7F_0 \rightarrow {}^5D_4$ (365 nm) and $^7F_0 \rightarrow {}^5G_6$ (375 nm) transitions of Eu(III). In this case the selection rules for the energy transfer process are satisfied. This is supported by Malta's theoretical model [28] and has also been analyzed by us [141].

Inspection of the data included in Table 2 shows significant similarities of the nephelauxetic effect (expressed by shifts of the $^5D_0 \rightarrow {}^7F_0$ transition) and the CF parameters (excluding B_2^4) for two compounds: $Eu(DPM)_3Phen$ and $Eu(TTFA)_3Nphen$. In this case two pairs of coupled ligands having different donor–acceptor properties lead to similar properties of the complexes. The intensities and distribution of the vibronic components are similar in the spectra of both compounds [121] (see Fig. 14 in [35]), consistent with the theory of vibronic transition probabilities [76,125].

The triplet states of the ligands can participate in the non-radiative quenching processes giving rise to back energy transfer from the $^5D_0$ excited state. An example is the complex with the Nphen ligand, which exhibits the lowest europium luminescence quantum yield. The second factor is the ligand-to-metal CT state. The efficiency of its participation in the degradation of the excitation energy of Eu(III) increases with the donor ability of the β-diketone radicals with weakening of the Eu–N bonds and corresponding strengthening of the Eu–O bonds [123].

Steric factors play a significant role in determining the structure of the compounds as demonstrated for a series of $Eu(DPM)_3$·Ph-related compounds, based on crystal field parameter calculations. Two groups of compounds with small and large Ph ligands have different luminescence spectra [122].

The dependence of the spectroscopic data on the ligands permits optimization of the properties of europium β-diketonates for their application in OLEDs. The most useful for this application seems to be $Eu(DPM)_3$·Ph and the fluorinated β-diketonates $Eu(TTFA)_3$·Ph, $Eu(OTOFOD)_3Ph$ (Ph – Phphen, Dphphen).

For the highly emitting $Eu(TTFA)_3$·5Mphen circularly polarized laser excitation generated a non-racemic excited state and circularly polarized luminescence (CPL) spectra were detected. This leads to the conclusion that enantiomeric structures exist in solution, and that the racemization rate is lower than the radiative rate in acetone solutions [126].

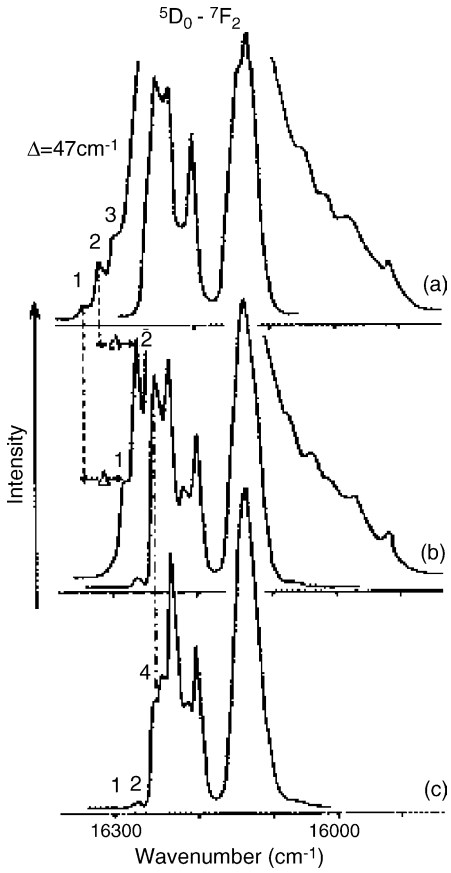

Fig. 12. Vibronic luminescence spectra of $Eu(TTFA)_3$·Bpy (a and b) and $Eu(TTFA)_3$·D-Bpy (c) at 77 K. Reprinted with permission from Ref. [124].*Copyright 2005 Elsevier Science*.

In the luminescence spectra of the Eu(III) β-diketonates investigated, a resonance effect has been discovered [121] (see Fig. 12). When vibronic sidebands of one of the electronic transitions of Eu(III) fall in the region of the zero-phonon lines of other transitions, redistribution of the intensities and slight shifts of the bands could occur. Thus the changes described above are the results of the generation of new vibronic states. One should use the nonadiabatic approximation in the quantum mechanical description of these systems [127,128].

The relative integral intensity of the vibronic sidebands of the Eu(III) electronic transitions, the intensity distribution in the sidebands, and the satellite vibration frequencies depend on the donor–acceptor properties of the ligands [25,30,35,121–23] and also on the sizes of the substituents of the ligands. This last has been demonstrated for a series of Eu(III) β-diketonates of formulae $Eu(\beta)_3$·Ph and $Eu(\beta)_3$·Bpy [124] (Figs. 13 and 14).

The intensities of the vibronic components increase with increasing covalency, thus confirming the theory of the vibronic transition probabilities as described in Section 1 (Eq. (1)). Moreover, in this case the non-radiative deactivation promoted by these phonons is also more effective.

Compounds with inner and outersphere 2,2′-bipyridine molecules, the first known complexes characterized in detail by X-ray diffraction, were synthesized and investigated: $LnWo_3$·Bpy(1/2Bpy) (1) [129], $EuWo_3Bpy$ (2) [130] (Wo = $CCl_3C(O)$

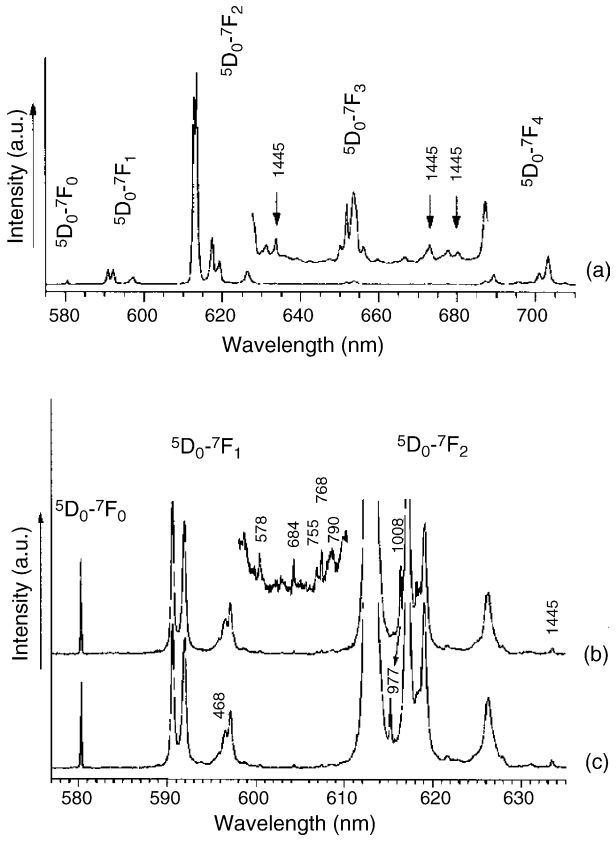

Fig. 13. Luminescence spectra of $Eu(CD_3COO)_3Bpy$ (a), $Eu(CH_3COO)_3Bpy$ (b) and $Eu(CH_3COO)_3D$-Bpy (c) in the region of $^5D_0 \rightarrow {}^7F_2$ transition at 77 K. Reprinted with permission from Ref. [128].*Copyright 2002 Elsevier Science*.

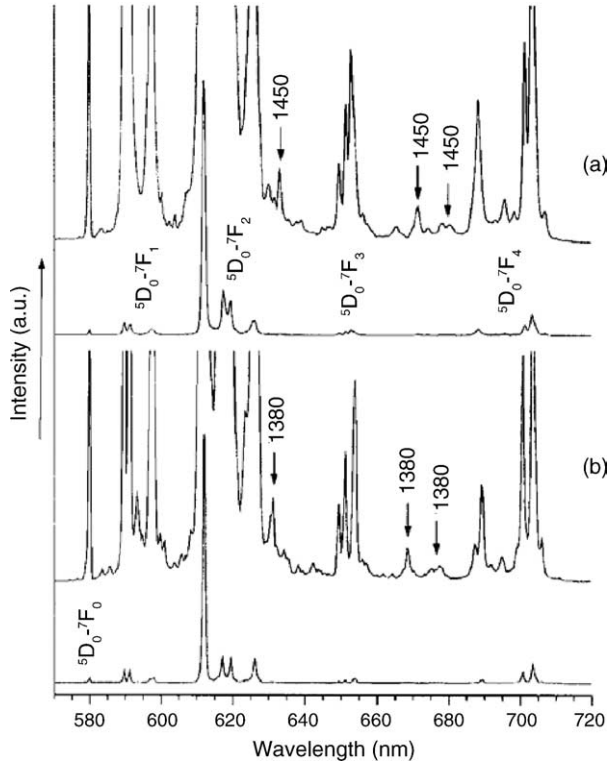

Fig. 14. Vibronic luminescence spectra of $Eu(TTFA)_3$·Nphen (a) and $Eu(DPM)_3$·Phen (b) at 77 K. Reprinted with permission from Ref. [124].*Copyright 2005 Elsevier Science*.

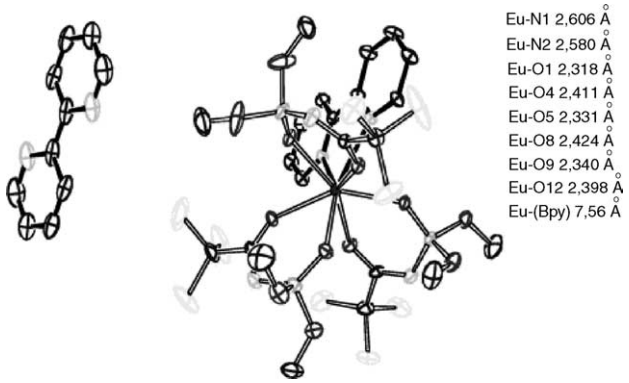

Fig. 15. Crystal structure of complex $Eu\beta_3Bpy(Bpy/2)$. Reprinted with permission from Ref. [35].*Copyright 2002 Elsevier Science*.

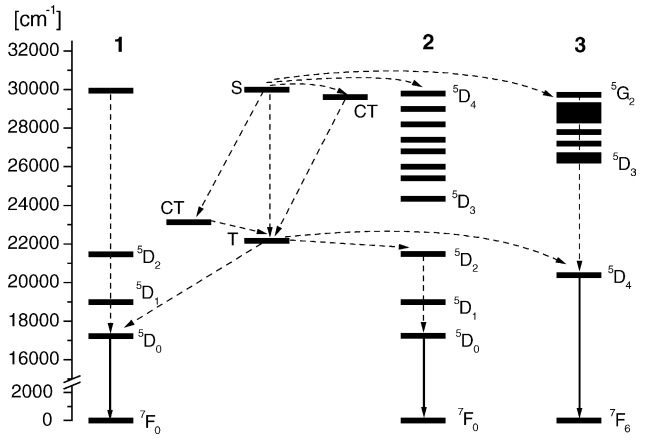

Fig. 16. The energy level diagrams of Eu(III) (1) and (2) systems and Tb(III) (2). The energy of the ligand singlet state was adopted from Harriman's report [145]. The location of the ligand triplet state was evaluated from phosphorescence spectrum of lanthanum respective complex.

$NP(O)(OCH_3)_2$), $[Eu(HFAA)_3Bpy{\cdot}H_2O]{\cdot}Bpy$ (3) (HFAA – hexafluoroacetone) [131] and $LnWo_3$·Phen (4) [132]. X-ray studies have shown the architecture of the mixed complexes (see Fig. 15 and Figs. 6 and 7 in [35]) with the non-coordinated 2,2′-bipyridine molecule located at different distances from the Eu(III). Compounds (1) and (3) differ in the type of β-diketone while the second ligand in both compounds is a 2,2′-bipyridine molecule, which allows us to analyze the effect of the β-diketone singlet and triplet states on the efficiency of the emission and the ligand-to-metal energy transfer.

If β-diketone is HFAA as in $[Eu(HFAA)_3Bpy{\cdot}H_2O]{\cdot}Bpy$ then, according to the X-ray data, the coordination number of Eu(III) is unexpectedly 9, involving a water molecule together with the organic ligands. Additional non-coordinating 2,2′-bipyridine molecules participate in the solid state and affect the emission efficiency. Thus, analysis of the energy transfer process through the inner- and outer-sphere Bpy molecules must take into account both the intra- and intermolecular energy transfer and migration of energy in the solid system [28,35].

Based on the spectroscopic data we have been able to construct the energy level diagram for both the Tb(III) and Eu(III) ions including the CT and ligand states (see Fig. 16). Energy can be transferred from the ligand singlet and triplet states directly

or by involving the Eu(III) CT state. Moreover, based on the decay time measurements, the relatively high $k_{nr}(T)$ rate constants determined for [Eu(HFAA)$_3$Bpy·H$_2$O]·Bpy point to the role of back-energy transfer and of the CT state in deactivation of the ligand states and their effect on the efficiency of the energy transfer. Direct energy transfer (involving the $^5D_1$ levels via the exchange mechanism and the $^5D_2$, $^5L_6$, $^5G_6$, $^5D_4$ levels via the multipolar mechanism) can occur. This is based on the location of the singlet and triplet states versus the metal levels for both systems investigated—as has been proposed by Malta's theoretical model [28,130,133].

Considering the energy of the CT states for both compounds, the role of the CT state in the energy transfer process seems to be more important for [Eu(HFAA)$_3$Bpy·H$_2$O]·Bpy [35]. In fact, deactivation of the lowest $^1\pi\pi^*$ level can follow various routes and the energy transfer from $^1\pi\pi^*$ to $^5D_0$ can occur, through different pathways, directly or via intersystem crossing to $^3\pi\pi^*$. Thus, the efficiency of the energy transfer can be defined as $\eta_{et} = \eta_{isc}\eta^3_{et}\pi\pi^*$ and the quantum yield is $\phi_{exp} = \eta_{isc}\eta^3_{et}\pi\pi^*\eta_r$.

In the emission spectra of LnWo$_3$ Bpy(1/2Bpy) a resonance effect has been observed. Most probably the coupled ν(P–N)*, ν(P–O)* and other modes [35] are responsible for the resonance conditions.

Lanthanide compounds with three types of β-diketones phosphoro-azo derivatives of the formulas Na[LnL$_4$]·H$_2$O [134,135] and LnC$_3$·2H$_2$O [136] (where L = Wo or Az; Wo = CCl$_3$–C(O)N–P(O)(OCH$_3$)$_2$; Az = C$_6$H$_5$–C(O)N–P(O)[N(CH$_2$)$_2$]$_2$; C = CCl$_3$–C(O)N–P(O)(NHC$_6$H$_5$)$_2$, Ln = Eu(III), Pr(III), Nd(III)) have been investigated in order to explain their structure and prove potential biological role. Substitution of the NP(O)(OCH$_3$)$_2$ ligand group by NP(O)N(CH$_2$)$_2$ changes the biological function of the compound. In vitro cytotoxicity experiments with lanthanide complexes exhibit their anticancer effect on the cell strains tested [135].

The comparative aspect of the f–f transition intensities with emphasis on their anisotropy and susceptibility to the electron–phonon coupling and the polarizability of the ligand has been the aim of our investigation of two series of lanthanide(III) (Nd, Eu, Pr) compounds of the formulae Ln(HX)$_3$(NO$_3$)$_3$ (**1**) and Ln(HX)$_3$Cl$_3$ (**2**) (where HX=CCl$_3$CO–NH–PO(Net$_2$)$_2$) [137,138].

Compounds having CN = 6 and 9 were investigated in the form of monocrystals. The D_3 symmetry for the compound (**1**) and most probably C_{2v} for the compound (**2**) were derived from the X-ray data and analysis of the electronic components in the low temperature (4 K) spectra. High, close to D_3, symmetry of the Pr(III) ion has been confirmed by the lack of the $^3H_4$ (A_1) → $^3P_0$ (A_1) components in the absorption spectrum of Pr(HX)$_3$Cl$_3$. Analysis of changes of the oscillator strength values of the hypersensitive transitions has showed that deformation of the structure increases in the series Pr–Nd–Eu with a decrease of the ionic radius.

As the compounds comprise the same organic ligand (HX) and the inorganic molecules, Cl^- and NO_3^-, it is clear that the latter are responsible for the crystal structure differences. The former can be considered as a source of the polarizability anisotropy. Intensities of the f–f transitions for the Pr(III) compound (**1**) are determined mainly by the strong electron–phonon coupling. These intensities are twice as small as compared to compound (**2**) and comparable with those reported by Richardson and others for high symmetry compounds [139]. The low temperature spectra confirm a strong vibronic contribution to the transition intensities. In fact, the strongest decrease of the intensities with decrease of temperature to 50 K has been observed in the $^3H_4 \rightarrow {}^3F_2$ transition. Most probably it is the result of the largest dynamic-to-static ratio found by Richardson for this transition in trigonal symmetry [140].

Values of the oscillator strengths of the electronic f–f transitions of the Pr(III) and Eu(III) compounds of the type (**1**) have been shown to be temperature and crystal orientation dependent and such relationships have been interpreted respectively in terms of contribution of the dynamic coupling and the polarizability mechanisms in the f–f transition intensities. Moreover, the Judd-Ofelt parameters calculated from the wide set of oscillator strengths of transitions in the absorption and emission spectra have been evaluated with considerable accuracy. It is quite unique—especially for the Pr(III) ion.

Analysis of the splitting of the components in the low temperature emission spectra of the Eu(HX)$_3$Cl$_3$ compound allows one to detect the resonance effect in the vibronic coupling.

Our aim has also been to obtain lanthanide β-diketonates pure and mixed with 1,10-phenanthroline trapped in silica or zirconia gels prepared by the sol–gel technique [141–144]. We have chosen the following complexes: Eu(AA)$_3$·2H$_2$O, Eu(BA)$_3$·2H$_2$O, Eu(AA)$_3$·Phen, Eu(BA)$_3$·Phen, NaNdWo$_4$·H$_2$O, Eu,Tb(Wo)$_3$L (L-Lewis base; 2,2′-bipyridine or Phen).

The structure of the precursor complexes controls the structure of the metal centers in the silica gel. Elimination of water from the precursor salts (during chelation) prevents water retention in the silica glasses [143]. The chelation also prevents aggregation of the dopant ions [142].

The Eu(III) chelates trapped in silica gel glass has been preserved and the complexes with phenanthroline exhibit more intense emission with longer decay times. The strongest emission has been observed for the Eu(BA)$_3$·Phen complexes trapped in silica gel glass obtained with acetone instead of alcohol. Its efficient emission points to the possibility of utilizing such material as luminescent devices for sensor applications. Intensity analysis of the emission spectra of the Eu(III) chelates allows one to investigate the structure of the metal centers in silica gel glass [142].

Lanthanide mixed chelates with phosphoro-azo-derivatives of β-diketonates (Wo) and 2,2′-bipyridine incorporated in zirconia glass thin films exhibit a distinct increase of the luminescence intensities of europium and terbium in the complexes as compared to the emission of lanthanide oxides in similar films [141]. This effect is a result of the efficient energy-transfer exchange between the ligand and the lanthanide as well as the increase of rigidity of the complex incorporated in zirconia glasses, which are more pronounced than for silica glass. These materials find wide application as light conversion molecular devices, organic layered electroluminescence diodes (OLEDs) and in fluorimetric techniques. This type of compound has also been used as a precursor in the synthesis of nanometer-range materials [146].

4. Photophysics of the lanthanide complexes applicable in biomedical assays

The design of efficient luminescent lanthanide-based probes for application in biological systems requires detailed knowledge concerning the efficiency of the ligand-to metal energy transfer, solution structure and dynamics, and the influence that these have on the important photochemical and photophysical properties. Within this broad area of research, energy transfer between identical chromophores has been the subject of numerous theoretical and experimental investigations [5–10,21,28,35,147–153].

Since the excited state energy transfer also has the effect of scrambling an initially photoselected orientational distribution, as measured by diminished linear polarization in the fluorescence from a rigid system (concentration depolarization), this phenomenon has also been used to probe the structure of polymer composites at the molecular level [154].

Of special interest are cage-like ligands containing aromatic *N*-oxide functional groups. The strong complexing ability of the cryptands results from their macrobicyclic nature, giving rise to a three-dimensional cavity well-fitted for the binding of cations. Lehn and co-workers developed strongly luminescent materials incorporating biheteroaromatic units such as 2,2′-bipyridine, bipyrimidine, 1,10-phenanthroline, 3,3′-biisoquinoline and later their *N*-oxides [5,7,147,155,156]. The heteroaromatic *N*-oxides are able to provide higher luminescence quantum yields than their *N*-heteroaromatic parents due to the stronger M-ligand interaction in spite of the presence of an additional decay process and lower molar absorption coefficient [147]. Eu(bpy.bpy.bpy) has been used in the TRACE/HTRF homogenous fluoroassay technique based on the FRET principles (FRET – fluorescence resonance energy transfer) [6]. The quantum yield has been increased by incorporating fluoride ions in the coordination sphere, allowing a total shielding through the formation of an ion pair [157]. The addition of carboxylic groups to two of the bipyridine units lead to a 2.5-fold increase of the cryptate fluorescence by shifting the absorption maximum wavelength and adapting to the nitrogen laser excitation at 337 nm. The substitution of bipyridine with one molecule of pyridine caused a dramatic decrease of the quenching process by decreasing the size of the cryptate cavity and prohibition of Eu(II) formation [158]. Also the $[Ln \subset bpy.bpy.py(CO_2Et)_2]^{3+}$ cryptates (Ln = Eu(III), Tb(III)) displayed relatively high emission quantum yields in aqueous solutions (14% and 25%). In this case the Tb(III) ion has energy levels more appropriate to give good resonant conditions with the triplet state of the cryptand [159]. Theoretical calculations revealed that the most probable channels involved in the luminescence process for Eu(III) are $So \Rightarrow S1 \Rightarrow T \Rightarrow (^5D_1, ^5D_0) \Rightarrow {}^7F_J$. The enhancement of the luminescence properties could be obtained by replacement of one pyridine nucleus by a five-membered ring inside the symmetrical trisbipyridine framework in the case of the terbium cryptate [160]. The luminescence induced by ligand excitation has been observed for Eu(III) and Tb(III) cryptates incorporating bpy or bpzpy chromophores in methanolic solutions [161].

One approach to obtaining highly emissive complexes is to employ flexible macrocyclic ligands capable of forming a suitable cavity for lanthanide ions and effectively eliminating solvent molecules from the first coordination sphere. The photophysical properties of europium and terbium podates with bpy or bipyridine-*N*,*N*′-dioxide subunits were studied in different solvents by Balzani et al. [162] and by Ziessel et al. [163,164]. The highest luminescence quantum yield of the Eu(III) podate was 0.35 in CH_3CN [163]. The triazacyclononane macrocycle with three negatively charged bipyridine carboxylate arms created very stable complexes with lifetimes of 1.85 and 0.5 ms and quantum yields of 12% and 10% for Eu(III) and Tb(III), respectively [164]. The X-ray structures for these complexes are known [165,166]. Detailed luminescence studies were carried out for the Gd(III), Eu(III) and Tb(III) complexes with a podand tris[3-(2-pyridylo-pyrazolyl] hydroborate in five solvents [167]. The respective X-ray structures have recently been published [168].

The structure, spectroscopy, photophysics and dynamics of the excited states of europium cryptates incorporating biisoquinoline dioxide ($biqO_2$) [151,152,169], lanthanide podate with bipyridine (bpy) [27,153,170–172] and the europium chelate with 2,2′-bipyridine-*N*-oxide ($bpyO_2$) [28,173,174] have been reported. Our interest has been to investigate the ligand-lanthanide energy transfer mechanism, the balance between forward and back energy transfer, the influence of complex structure on photophysical properties as well as the use of CPE/CPL techniques to study the dynamics of the excited state. Incorporation of racemic lanthanide complexes into silica gels obtained by the sol–gel method is a useful technique for racemization elimination, and thus allows one to probe individual enantiomers by circularly polarized excitation (CPE) followed by circularly polarized luminescence (CPL) [50,175–177].

Three cryptates incorporating one 3,3′-biisoquinoline-2,2′-dioxide ($biqO_2$) unit (labeled $Ln \subset 1$, where Ln = Eu(III), Tb(III), Gd(III) and three $biqO_2$ units (labeled $Eu \subset 2$), three $biqO_2$ units with three N atoms (labeled $Eu \subset 3$) have been studied [151,152,169]. The $[Eu \subset (biqO_2.2.2)(CF_3SO_3)]_3 \cdot CH_3CN \cdot H_2O$ ($Eu \subset 1$) forms rhombic crystals with space group *Pbca*. The unit cell of dimensions $a = 12.831(3)$, $b = 24.265(5)$, $c = 29.252(6)$ Å and $\alpha = \beta = \gamma = 90^\circ$ consists of eight formula units [151]. As expected, all of the oxygen and nitrogen atoms of the cryptand are involved in the metal ion coordination. As can be seen in Fig. 17, a surprising result, compared to the known structures of lanthanide cryptates [178–183], is that the coordination number of Eu(III) in this solid complex is 10. Two oxygen atoms from one of the triflate counter ions are also coordinated. Because the bound triflate oxygen atoms are aligned almost perpendicular to the bound *N*-oxide oxygen atoms, the Eu(III) environment is very close to C_2 symmetry. However, in the analysis of the electronic transitions for lanthanide(III) ions it is often the case that a reasonable analysis can be derived by consideration of only the coordinated atoms. Under this assumption, the site symmetry may be approximated by C_{2v} what is confirmed by the emission spectrum at 77 K (see Fig. 18). The ab initio SCF calculations have been made because the differences between photophysical properties (see

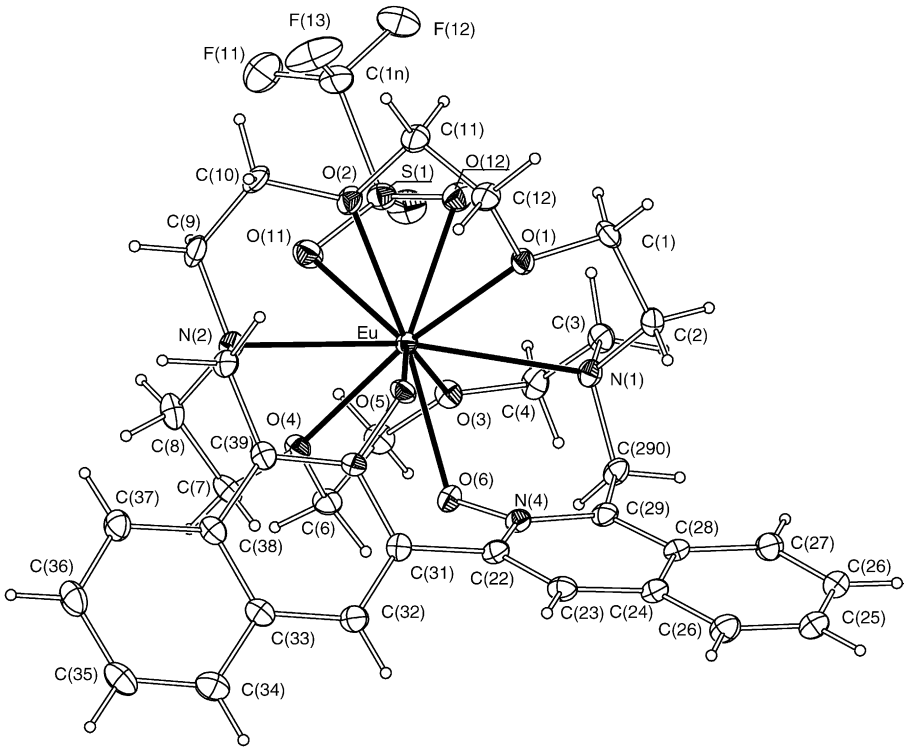

Fig. 17. The molecular structure of $[Eu \subset (biqO_2.2.2)(CF_3SO_3)](CF_3SO_3)_2 \cdot CH_3CN \cdot H_2O$ ($Eu \subset 1$). Reprinted with permission from Ref. [151].*Copyright 2000 American Chemical Society*.

Table 3) of the three types of cryptates require the knowledge of the cryptates structures. Since the RHF calculations of $Y \subset 1$ reproduce well the X-ray data structure of $Eu \subset 1$, this same approach has been applied for the molecular structure modeling of the next two cryptates [152]. The structures created in the complexes with ligand 2 and 3 show elongation of the cryptand molecules 3. The N3–N4 (where N3 and N4 are cryptand nitrogen atoms) distance is very long (7.640 Å) in cryptand 2 but becomes shorter in the $Eu \subset 2$ complex (5.875 Å) indicating participation of the nitrogen atoms in coordination. M–N3 bond lengths are equal to 2.937 Å showing very weak bonding. On the other hand, for $Eu \subset 3$ this elongation is more significant and the N3–N4 distance is 10.121 Å after complexation as compared to 10.742 Å in the cryptand. One can expect that further elongation of the ligand molecule should lead to a change of the cage inside cryptate enabling additional metal penetration of the coordination sphere by solvent molecules and/or counterions (see Table 3). It can also create new pathways of de-excitation of the lanthanide emission, since the metal ion can move from site to site. Moreover, the size of this cage is sufficient to host two metal ions inside the cryptand 3. Fig. 19 presents the emission spectra of $Eu \subset 2$ and $Eu \subset 3$ under different conditions. The

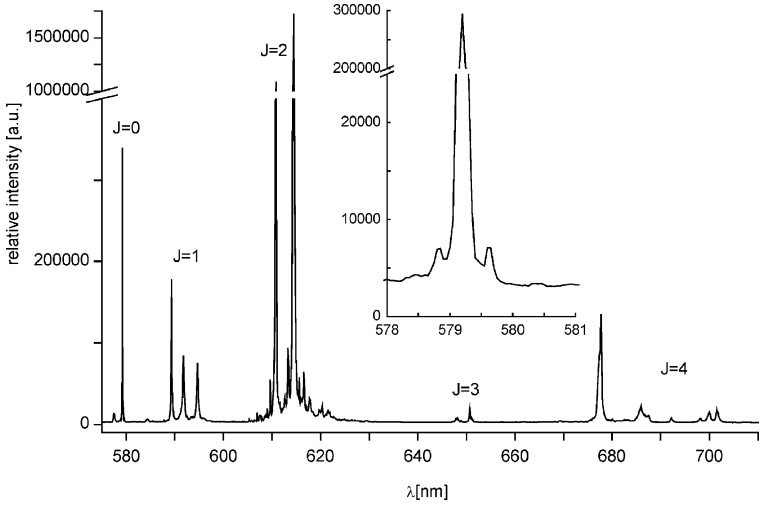

Fig. 18. Luminescence spectrum of $Eu \subset 1$ solid state at 77 K. The insert is an enlargement $^5D_0 \rightarrow {}^7F_0$ transition [151]. Reprinted with permission from Ref. [151].*Copyright 2000 American Chemical Society*.

Table 3
Selected experimental decay rate constants for Eu ⊂ 1, Eu ⊂ 2 and Eu ⊂ 3

Compounds	$k_{r,n}$[a] (s^{-1})	$k_{nr}(OH)$[b] (s^{-1})	$k_{nr}(T)$[c] (s^{-1})	$\sum k$ (s^{-1})	$n(H_2O)$[d]	Quantum yield (%) experimental	Quantum yield (%) calculation
Eu ⊂ 1	1243	1270	463	2976	1.36	21.5[e] (77 K)	18 (77 K)
Eu ⊂ 2	3125	2698	4870	7142	2.96		
Eu ⊂ 3	4545	2820	3571	5000	2.90		

[a] Defined as $1/\tau(D_2O)_{77\,K}$, where $k_{r,n} = k_r + k_{nr}$(other vibrations).
[b] Defined as $1/\tau(H_2O)_{300\,K} - 1/\tau(D_2O)_{300\,K}$.
[c] Defined as $1/\tau(D_2O)_{300\,K} - 1/\tau(D_2O)_{77\,K}$.
[d] Average number of coordinated water molecules [17].
[e] $Ru(bpy)_3^{2+}$ was taken as reference for the quantum yield measurement.

luminescence spectra manifest modification of the structures of the europium cryptates of both types. Moreover, in the solid-state spectrum of Eu ⊂ 2 at 77 K broadening of the bands is observed that can indicate disordering of the system at low temperatures. Because a decrease of temperature leads to decrease of the volume, the transformation of the structure where the M–N bonding still exist (according to the RHF calculations) is rather difficult. In Eu ⊂ 3 the M–N bonding is not formed and broadening of the emission lines is not observed [152]. Some photophysical data are reported in Table 3.

Both ligand-to-metal charge transfer (LMCT) states and ligand $^3\pi\pi^*$ states control the energy transfer processes in these complexes. The strong temperature dependence of the luminescence lifetime reflected in $k_{nr}(T)$ for Eu ⊂ 2 and Eu ⊂ 3 suggests that the LMCT states also take part in the non-radiative deactivation of excited Eu(III). Structural crystallographic data for Eu ⊂ 1, electronic structure calculations and theoretical models have been used to obtain the intramolecular energy transfer rates. There are five states that show appropriate resonance conditions with the ligand excited states. The choice of $^5D_0$, $^5D_1$, $^5D_2$, $^5G_6$ and $^5D_4$ results from the favourable resonance conditions and from the selection rules stemming from the theoretical models [21,152,184]. According to these selection rules direct energy transfer to the $^5D_0$ level is not allowed. This rule is, however, relaxed due to the J-mixing effects and the thermal population of the $^7F_1$ level. Table 4 presents the energy transfer and back-transfer rates for the Eu ⊂ 1 cryptate. The arrows

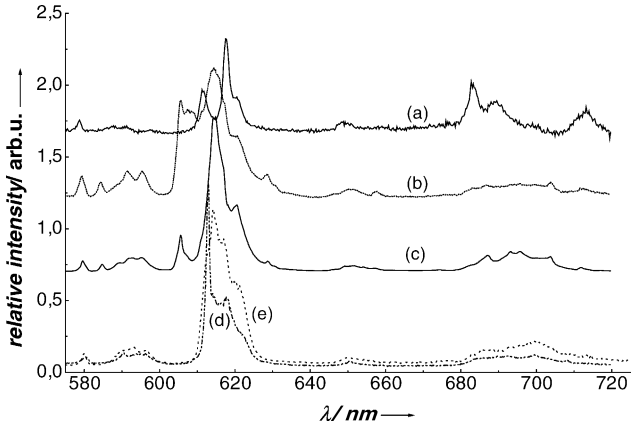

Fig. 19. The luminescence spectra of Eu⊂2 (a) solid at 293 K, (b) solid at 77 K, (c) in CH_3CN at 77 K and Eu⊂3 (d) solid at 77 K, (e) in CH_3CN at 77 K. Reprinted with permission from ref. [152].*Copyright 2004 Wiley-VCH*.

Table 4
Calculated energy transfer rates for Eu ⊂ 1

Ligand state (cm^{-1})	4*f* state (cm^{-1})	Transfer rate (s^{-1})	Back-transfer rate (s^{-1})
Triplet (18018) →	$^5D_0$ (17300)	$k_{28} = 1.96 \times 10^7$	$k_{82} = 31.83$
Triplet (18018) ←	$^5D_1$ (19000)	$k_{72} = 3.34 \times 10^8$	$k_{27} = 4.04$
Triplet (18018) ←	$^5D_2$ (21500)	$k_{62} = 2.82 \times 106$[a]	$k_{26} \approx 0$
Singlet (29010) →	$^5G_6$ (26750)	$k_{35} = 4.41 \times 106$[b]	$k_{53} \approx 0$
Singlet (29010) →	$^5D_4$ (27600)	$k_{34} = 1.66 \times 106$[b]	$k_{43} \approx 0$

[a] Dipolo–2^1 polo mechanism.
[b] Dipole–dipole mechanism.

indicate the direction of the energy transfer. The energy transfer rate is larger for the $^5D_1$ level, for which the exchange mechanism dominates. An insignificant back-transfer rate is observed, due to the low temperature (77 K) and the finite energy mismatch Δ (>1500 cm^{-1}) that leads to a small Boltzmann factor $e^{-|\Delta|/k_BT}$. Typical values of the remaining transfer rates were assumed to be identical to those found for other coordination compounds, namely, $k_{13} = \phi = 10^4$, $k_{21} = 10^5$, $k_{32} = 10^8$, and $k_{31} = 10^6\ s^{-1}$ [21].

An additional quenching mechanism was investigated by considering a low-lying ligand-to-metal-charge-transfer state (LMCT). Therefore, three situations could be taken into account: (a), (b) are presented in Fig. 20 and (c) the LMCT state is not considered and only eight states involved in the energy transfer process should be applied. The quantum yields and the decay lifetimes were obtained from these results and compared to the experimental data (Table 3). Comparison of the experimental quantum yields with the calculated ones shows that the LMCT state, located close to the ligand singlet state, is involved in the energy transfer process. According to the selection rules derived for the energy transfer process, the $^3\pi^* \rightarrow {}^5D_1$ transition is allowed by the exchange mechanism as described by Eq. (2):

$$W_{ET} = \frac{8\pi}{3\hbar}\frac{e^2(1-\sigma_0)^2}{(2J+1)R_L^4}F\langle\alpha' J'\|S\|\alpha J\rangle^2 \times \sum_m \left|\left\langle \phi \left| \sum_k \mu_z(k) s_m(k) \right| \phi' \right\rangle\right|^2 \quad (2)$$

where F is the so-called energy mismatch factor which can be calculated from the approximate expression given by Malta [184], S the total spin operator (in units of $\hbar$) of the lanthanide ion, μ_z the z component of the electric dipole operator, s_m

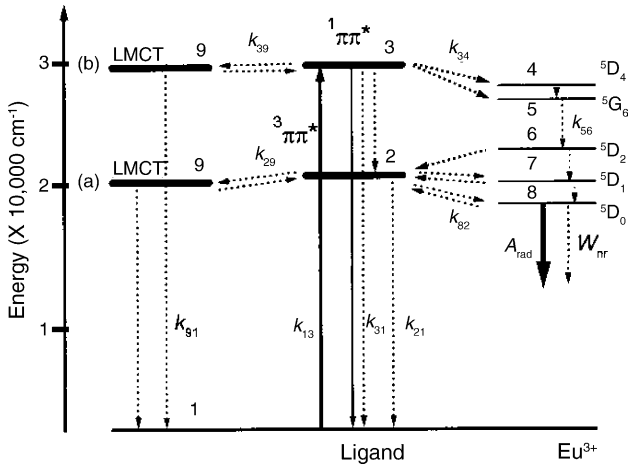

Fig. 20. Diagram of the most probable states to be involved in the energy transfer process in Eu⊂1, with their numbering scheme. The solid and dashed arrows represent radiative rate(A_{rad}) and non-radiative rate (W_{nr}) processes, respectively. The diagram also shows how the MCT state is taken into consideration: close to (a) the triplet and (b) the singlet states of the ligand. Reprinted with permission from ref. [152].*Copyright 2004 Wiley-VCH*.

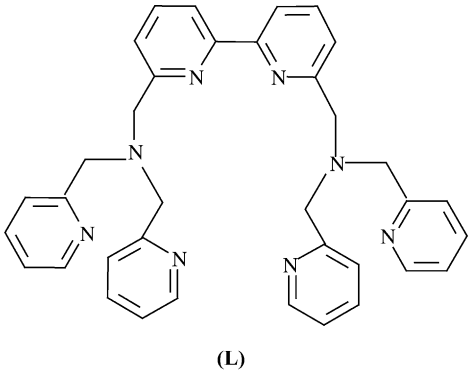

(L)

6,6'-bis[bis(2-pyridylmethyl)aminomethyl]-2,2'-bipyridine

Fig. 21. Structural formula of the podant (L) [153].

Table 5
Luminescence decay times (ms) for TbL and EuL in the solid state and in various solutions at 293 and 77 K

	TbL				EuL			
	293 K		77 K		293 K		77 K	
	τ_H	τ_D	τ_H	τ_D	τ_H	τ_D	τ_H	τ_D
CH_3OH	1.5	1.67	1.8	2.93	0.94, 0.33	1.26, 0.34		1.52
H_2O	1.53	1.76						
CH_3CN	1.4		1.35				1.01	
Solid	1.4		1.78		0.54, 0.06			

the spherical component of the spin operator for the ligands electrons, σ_0 the screening factor due to the filled 5s and 5p sub-shells of the lanthanide ion, and R_L is the distance from the lanthanide ion to the region of the ligand molecule in which the ligand donor (or acceptor) state is localized.

Investigation of the pressure effect on the luminescence has shown little change in the coordination of Eu(III) in the cryptand but a very substantial increase in the population of the $^5D_0$ state, either due to an increase in the energy transfer from the ligand triplet state or a decrease in the back-transfer deactivation [151]. As a first approximation, a small decrease in the distance from the ligand to the metal ion would be expected to increase both the forward and reverse energy transfer, although not necessarily equally. More interestingly, increased pressure is known to have a pronounced effect on the energy of the ligand π-orbitals, so the effect that we observe may be due to the changes in the metal:ligand orbital overlap. This kind of compound in which the luminescence intensity depends strongly on pressure because of the existence of competitive energy transfer processes controlled by the energy gap, can be very useful for potential pressure sensors designs.

The investigation of lanthanide(III) complexes with the podand 6,6′-bis[bis(2-pyridylmethyl)aminomethyl]-2,2′-bipyridine (L) (Fig. 21) has illustrated the quality and quantity of information on the energetics, the solution structure, and the photophysics that is now available for the characterization of luminescent lanthanide complexes in solids and solutions [27,153,170–172]. For TbL and EuL there exists a very efficient ligand-to-metal energy transfer. For EuL the participation of LMCT in the quenching of the emission has been predicted based on the excitation spectra, the quantum yields and the measured decay rate constants. The partial photophysical data are presented in Table 5.

The energy gap between the ligand triplet state (21 929 cm^{-1}) and the Tb(III) $^5D_4$ and the Eu(III) $^5D_0$, $^5D_1$ states are 1438, 4681 and 2899 cm^{-1}, respectively. This allows one to estimate the efficiency of the phonon-assisted energy transfer. Comparing the spectra for the solid state and the solutions in the range of the $^5D_0 \rightarrow {}^7F_0$ transition we associate these two peaks with the $[Eu(L)Cl_2]^+$ (**A**) and $[Eu(L)Cl]^{2+}$ (**B**) forms of the Eu(III) complex [172]. ΔV, which denotes the difference in volume between the products and the reactants may be obtained from a plot of the natural log of the ratio of the peak areas versus pressure. The results are shown in Fig. 22. The positive value of ΔV

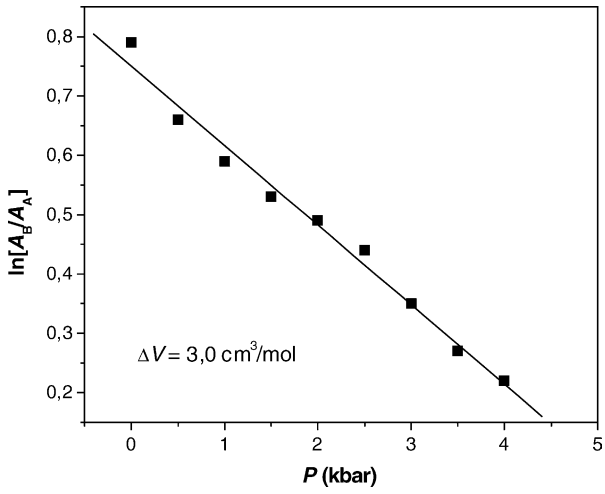

Fig. 22. A plot of the measured luminescence dissymmetry factor, g_{lum}, measured at 543 nm vs. temperature for a solution of TbL in methanol. Reprinted with permission from ref. [153].*Copyright 2000 Elsevier Science*.

(3.0 cm^3/mol) means that the formation of the **A** complex, having lower net charge is stimulated by increasing pressure. This result is consistent with the effects of solvent electrostriction in which lower charged species are preferred at high pressure due to the decreased solvent alignment. Measurements of circularly polarized luminescence (CPL) from a solution of the Dy(III) complex following circularly polarized excitation confirms the chiral structure of the complexes under study. No CPL is present in the luminescence from the Eu(III) or Tb(III) complex because of efficient racemization. This technique is only successful if the non-racemic excited state population is maintained during the excited state lifetime [50]. Although generally not as luminescent as Tb(III) or Eu(III) in solution, there has been some interest in studying the visible luminescence from complexes containing Dy(III), since the lifetime of this ion is of the order of microseconds, allowing one to probe shorter time scales. For the first time variations in CPL can be used to investigate the temperature dependence of non-racemic equilibria. Increase of temperature leads to an unexpected (linear) increase of the dissymmetry factor [153]. The data are consistent with an equilibrium between a solvent penetrating the first coordination sphere and the dissociated structure. It makes sense that at increased temperature formation of the dissociated species is increased, although no structural evidence for this identification is possible. The results are a part of an overall effort to develop specific sensitive luminescent sensors using the lanthanide(III) ions. Of special interest is the exploitation of chiral discrimination in this research area, detecting differences in the magnitude of the circularly polarized luminescence. Encapsulation of luminescent lanthanide ions in chiral podands which are designed to interact with target functional groups, and that contain properly selected absorption chromophores, show great potential to produce useful systems.

The applications of CPL spectroscopy to lanthanide complexes with DPA (dipicolinic acid), bypO$_2$ (2,2′-bipyridine-*N*-oxide), PEDPA (4-phenyl-ethynyl-dipicolinic acid) and podand (6,6′-bis[bis(2-pyridylmethyl)aminomethyl]-2,2′-bipyridine) embedded in rigid gels have been reported [27,175–177]. At high concentrations, however, the effect of the excited state racemization cannot be neglected because of the resonance energy transfer occurring between the opposite enantiomers. This is the first experimental observation of this phenomenon [175]. This area of research has the potential to provide unique information concerning differences in diastereomeric energy transfer rates.

The kinds of experiments mentioned above are inherently sensitive to the nature of the local environment of the complexes in sol–gel matrices, and this is the focus of the results presented here. Such information is critical for the continuous development of sol–gel based sensors.

Acknowledgment

The work was partly supported by the National Science Fundation (USA), by the European Union; Marie Curie program and Polish National Science Committee (KBN).

References

[1] T. Justel, J.-C. Krupa, D. Wiechert, J. Lumin. 93 (2001) 173.
[2] M.F. Reid, L. van Pieterson, R.T. Wegh, A. Meijerink, Phys. Rev. B 62 (2000) 14744.
[3] P. Dorenbos, Phys. Rev. B. 62 (2000) 15650.
[4] J.-C.G. Bünzli, in: J.-C.G. Bünzli, G.R. Choppin (Eds.), Lanthanide Probes in Life, Chemical and Earth Science, Elsevier, Amsterdam, 1989, p. 219.
[5] N. Sabbatini, M. Guardigli, I. Manet, R. Ungaro, A. Casnati, R. Ziessel, G. Ulrich, Z. Asfari, J.-M. Lehn, Pure Appl. Chem. 67 (1995) 135.
[6] H. Bazin, E. Trinquet, G. Mathis, Rev. Mol. Biotechnol. 82 (2002) 233.
[7] B. Alpha, V. Balzani, J.-M. Lehn, S. Perathoner, N. Sabbatini, Angew. Chem. Int. Ed. Engl. 26 (1987) 1266.
[8] H. Mikola, H. Takkalo, I. Hemmilä, Bioconj. Chem. 6 (1995).
[9] V.M. Mukkala, J.J. Kankare, Helv. Chim. Acta 75 (1992) 1578.
[10] W.W. De Horrocks Jr., P. Bolender, W.D. Smith, R.M. Supkowski, J. Am. Chem. Soc. 119 (1997) 5972.
[11] J.-C.G. Bünzli, C. Piquet, Chem. Rev. 102 (6) (2002) 1897.
[12] H. Tsukube, S. Shinoda, Chem. Rev. 102 (2002) 2389.
[13] K. Wong, R. Li, Y. Cheng, B. Zhu, Coord. Chem. Rev. 190 (1999) 297.
[14] D. Parker, R.S. Dickins, H. Puschmann, C. Crossland, S.A.K. Howard, Chem. Rev. 102 (2002) 1977.
[15] E. Nieboer, Struct. Bonding (Berlin) 22 (1975) 1.
[16] F.S. Richardson, Chem. Rev. 541 (1982).
[17] W.D. Horrocks Jr., Adv. Inorg. Bioch. 4 (1982) 201, and references cited therein;
W.D. Horrocks Jr., M. Albin, Progr. Inorg. Chem. 31 (1984) 1, and references cited therein.
[18] J. Legendziewicz, E. Huskowska, in: B. Jeżowska-Trzebiatowska, J. Legendziewicz, W. Stręk (Eds.), Application of Luminescence in Studies of Ln(III) Ions Interaction with Aminoacids; in Excited States of Transition Elements, World Scientific Publishing Co. Pte. Ltd, Singapore, 1989, p. 228, and references cited therein.
[19] Z. Zheng, Chem. Commun. (2001) 2521.
[20] A. Roig, R. Hettich, H.J. Schneider, Inorg. Chem. 37 (1998) 751.
[21] G.F. de Sá, O.L. Malta, C. De Mello Donegá, A.M. Simas, R.L. Longo, P.A. Santa-Cruz, E.F. da Silva Jr., Coord. Chem. Rev. 196 (2000) 165.
[22] J.-C. Krupa, M. Queffelec, J. Alloys Compd. 250 (1997) 287.
[23] R.T. Wegh, A. Meijerink, Phys. Rev. B. 60 (1990) 10820.
[24] C.R. Ronda, J. Alloys Compd. 225 (1995) 534.
[25] V. Tsaryuk, J. Legendziewicz, V. Zolin, L. Puntus, J. Sokolnicki, in: P. Vincenzini (Ed.), Proceedings of Ninth CIMTEC, World Forum on New Materials: Advances in Science and Technology, vol. 27, Techna Srl Faenza, Italy, 1999, p. 299.
[26] D. Parker, P. Kanthi-Senanayake, J.A.G. Williams, J. Chem. Soc, Perkin Trans. 2 (1998) 2129.
[27] J. Sokolnicki, R. Wiglusz, S. Radzki, A. Graczyk, J. Legendziewicz, Opt. Mater. 26 (2004) 199.
[28] O.L. Malta, J. Legendziewicz, E. Huskowska, I. Turowska-Tyrk, R.Q. Albuqerque, C. De Mello Donegá, F.R.G. e Silva, J. Alloys Compd. 323–324 (2001) 654.
[29] J. Kido, Y. Okamoto, Chem. Rev. 102 (2002) 2357.
[30] V. Tsaryuk, V. Zolin, J. Legendziewicz, J. Sokolnicki, V. Kudryashova, Proceedings of 11th International Workshop on Inorganic and Organic Electroluminescence, September 23, Ghent, Belgium, 2002.
[31] J. Legendziewicz, in: W. Stręk, W. Ryba-Romanowski, J. Legendziewicz, B. Jeżowska-Trzebiatowska (Eds.), Spectroscopy of Dimeric and Polymeric Ln(III) Compounds Single Crystals; in Excited States of Transition Elements, World Scientific Publishing Co. Pte. Ltd, Singapore, 1992, p. 149.
[32] H. Tsukube, S. Shinda, H. Temiaki, Coord. Chem. Rev. 190 (1999) 297.
[33] P. Li, D.S. Ma, C. Higginbotham, T. Hoffman, A.R. Ketring, C.S. Cutter, S.S. Jurisson, Nucl. Med. Biol. 28 (2001) 145.

[34] D.E. Reichert, S.S. Lewis, C.J. Anderson, Coor. Chem. Rev. 184 (1999) 3.
[35] J. Legendziewicz, J. Alloys Compd. 300–301 (2000) 71;
J. Legendziewicz, J. Alloys Compd. 341 (2002) 34, and references cited therein.
[36] R.S. Dickins, A.S. Batsanov, J.A.K. Howard, D. Parker, H. Puschmann, S. Salamano, Dalton Trans. (2004) 70.
[37] W.D. Horrocks, D.R. Sudnick, J. Am. Chem. Soc. 101 (1979) 2;
W.D. Horrocks Jr., D.R. Sudnick, Acc. Chem. Res. 14 (1981) 384.
[38] M. Albin, W.D. Horrocks Jr., Inorg. Chem. 24 (6) (1985) 895.
[39] T. Głowiak, J. Legendziewicz, E. Huskowska, P. Gawryszewska, Polyhedron 15 (17) (1996) 2939.
[40] E. Huskowska, J. Legendziewicz, Polyhedron 12 (19) (1993) 2387.
[41] J. Legendziewicz, Z. Ciunik, P. Gawryszewska, J. Sokolnicki, J. Alloys Compd. 225 (1995) 372.
[42] J. Legendziewicz, Z. Ciunik, P. Gawryszewska, J. Sokolnicki, Polyhedron 18 (1999) 2701.
[43] H.G. Brittain, Inorg. Chim. Acta 18 (7) (1979) 1740.
[44] H.G. Brittain, Coord. Chem. Rev. 48 (3) (1998) 243.
[45] J. Legendziewicz, W. Stręk, E. Huskowska, T. Kim-Anh, in: B. Jeżowska-Trzebiatowska, J. Legendziewicz, W. Stręk (Eds.), Excited States of Transition Elements, World Scientific Publishing Co. Pte. Ltd, Singapore, 1989, p. 258.
[46] J. Sztucki, W. Stręk, in: B. Jeżowska-Trzebiatowska, J. Legendziewicz, W. Stręk (Eds.), Excited States of Transition Elements, World Scientific Publishing Co. Pte. Ltd, Singapore, 1989, p. 528.
[47] O.E.R. Birnbaum, D.W. Darnall, Bioinorg. Chem. 3 (1973) 15.
[48] A.D. Sherry, C. Yoshida, E.R. Birnbaum, D.W. Darnall, J. Am. Chem. Soc. 95 (1973) 3011.
[49] G. Bobba, R.S. Dickins, S.D. Kean, C.E. Mathieu, D. Parker, R.D. Peacock, G. Siligardi, M.J. Smith, A.G. Williams, C.F.G.C. Geraldes, J. Chem. Soc., Perkin Trans 2 (2001) 1729.
[50] J.P. Riehl, G. Muller, in: K.A. Gschneidner Jr., J.-C.G. Bünzli, V.K. Pecharsky (Eds.), Circularly Polarized Luminescence Spectroscopy from Lanthanide Systems in Handbook on the Physics and Chemistry of Rare Earths, vol. 34, Amsterdam, 2005, p. 289 (Chapter 220).
[51] B.R. Judd, Phys. Rev. 127 (1962) 750.
[52] J.J. Dallara, M. Reid, F.S. Richardson, J. Phys. Chem. 88 (1984) 3587.
[53] C. Kremer, J. Torres, S. Dominguez, A. Mederos, Coord. Chem. Rev. (2004).
[54] R. Wang, H.D. Selby, H. Lin, M.P. Arducci, T. Sin, Z. Zheng, J.W. Anthis, R.S. Staples, Inorg. Chem. 41 (2002) 278.
[55] R. Wang, Z. Zheng, T. Sin, R. Staples, Angew. Chem. Int. Ed. 38 (1999) 1813.
[56] E. Huskowska, I. Turowska-Tyrk, J. Legendziewicz, T. Głowiak, J. Alloys Compd. 852 (1998) 275–277.
[57] J. Legendziewicz, T. Głowiak, E. Huskowska, C.N. Dao, Polyhedron 8 (1989) 2139.
[58] J. Legendziewicz, T. Głowiak, E. Huskowska, C.N. Dao, Polyhedron 7 (1988) 2495.
[59] C.N. Dao, E. Huskowska, T. Głowiak, J. Legendziewicz, J. Less-Common. Met. 136 (1988) 339.
[60] T. Głowiak, J. Legendziewicz, C.N. Dao, E. Huskowska, J. Less-Common. Met. 168 (1991) 237.
[61] I. Csöregh, E. Huskowska, J. Legendziewicz, Acta Cryst. C 48 (1992) 1030–1033.
[62] I. Csöregh, P. Kierkegaard, J. Legendziewicz, E. Huskowska, Acta Chim. Scand. A 41 (1987) 453;
I. Csöregh, P. Kierkegaard, J. Legendziewicz, E. Huskowska, Acta Chim. Scand. A 43 (1989) 636.
[63] I. Csöregh, M. Czugler, P. Kierkegaard, J. Legendziewicz, E. Huskowska, Acta Chem. Skand. 43 (1989) 735.
[64] I. Csöregh, P. Kierkegaard, J. Legendziewicz, E. Huskowska, Acta Chem. Skand. 43 (1989) 636.
[65] J. Legendziewicz, H. Kozłowski, B. Jeżowska-Trzebiatowska, E. Huskowska, Inorg. Nucl. Chem. Lett. 15 (1979) 349;
J. Legendziewicz, E. Huskowska, H. Kozłowski, B. Jeżowska-Trzebiatowska, Inorg. Nucl. Chem. Lett. 17 (1981) 57.
[66] J. Legendziewicz, E. Huskowska, A. Waśkowska, Gy. Argay, Inorg. Chim. Acta 92 (1984) 151;
J. Legendziewicz, E. Huskowska, A. Waśkowska, Gy. Argay, Inorg. Chim. Acta 95 (1984) 57.
[67] J. Legendziewicz, E. Huskowska, Gy. Argay, A. Waśkowska, J. Less-Common. Met. 146 (1989) 33.
[68] T. Głowiak, C.N. Dao, J. Legendziewicz, E. Huskowska, Acta Cryst. C 47 (1991) 78–81.
[69] J. Legendziewicz, P. Gawryszewska, E. Gałdecka, Z. Gałdecki, J. Alloys Compd. 275–277 (1998) 356;
J. Legendziewicz, P. Gawryszewska, E. Gałdecka, Z. Gałdecki, New J. Chem. 24 (2000) 387.
[70] J. Legendziewicz, P. Gawryszewska, E. Gałdecka, Z. Gałdecki, J. Lumin. 72–74 (1997) 559;
J. Legendziewicz, P. Gawryszewska, E. Gałdecka, Z. Gałdecki, Less-Common Met. 136 (1988) 339.
[71] E. Gałdecka, Z. Gałdecki, P. Gawryszewska, J. Legendziewicz, New J. Chem. 22 (1998) 941.
[72] T. Głowiak, E. Huskowska, J. Legendziewicz, Polyhedron 10 (1991) 175–178.
[73] J. Legendziewicz, Wiadomości Chemiczne 42 (1988) 605.
[74] W. Wojciechowski, J. Legendziewicz, M. Puchalska, Z. Ciunik, J. Alloys Compd. 380 (2004) 285.
[75] M. Zimmer, Chem. Rev. 102 (2002) 759.
[76] G. Blasse, Inorg. Chim. Acta 167 (1990) 33, and references cited therein.
[77] T. Głowiak, E. Huskowska, J. Legendziewicz, Polyhedron 11 (22) (1992) 2897.
[78] S. Natarayan, L.K.M. Rao, J. Inorg. Nucl. Chem. 43 (1981) 1693.
[79] G.L. Einspahr, G.L. Garland, G.E. Bugg, Acta Cryst. B 33 (1977) 3385.
[80] D. Van Der Helm, T.V. Willoughby, Acta Cryst. B 25 (1969) 2317.
[81] B. Holmquist, Adv. Inorg. Bioch. 2 (1980) 75.
[82] C.W. Tang, S.A. Van Slyke, Appl. Phys. Lett. 51 (1987) 2902.
[83] J.H. Burroughes, D.D.C. Bradley, A.R. Brown, R.N. Marks, K. Mackay, R.H. Friend, P.L. Burns, A.B. Holmes, Nature 347 (1990) 539.
[84] C.Y. Wang, Z.J. Yang, Y. Li, L.W. Gong, G.W. Zhao, Phys. Status Solidi A 191 (2002) 117.
[85] A.J. Kenyon, Progr. Quantum Electron. 26 (2002) 225.
[86] W. Zhou, Q. Jiang, Z. Lu, X. Wie, M. Xie, D. Zou, T. Tsutsui, Synth. Met. 111–112 (2000) 445.
[87] Zuqiang Bian, Deqing Gao, Kezhi Wang, Linpei Jin, Chunhui Huang, Thin Solid Films 460 (2004) 237.
[88] E. Stathatos, P. Lianos, E. Evgeniou, A. Keramidas, Synth. Met. 139 (2003) 433.
[89] Y.J. Fu, T.K.S. Wong, Y.K. Yan, G.M. Wang, X. Hu, Thin Solid Films 417 (2002) 78.
[90] Y.J. Fu, T.K.S. Wong, Y.K. Yan, X. Hu, J. Alloys Compd. 358 (2003) 235.
[91] R. Reyes, M. Cremona, E.E.S. Teotonio, H.F. Brito, O.L. Malta, Thin Solid Films 22 (2004) 59.
[92] Y. Zheng, J. Lin, Y. Liang, Q. Lin, Y. Yu, S. Chuan Guo, H. Wang, Zhang, Mater. Lett. 54 (2002) 424.
[93] X. Du, J. Hou, H. Deng, J. Gao, J. Kang, Spectrochim. Acta Part A 59 (2003) 271.
[94] R.J. Curry, W.P. Gillin, Synth. Met. 111–112 (2000) 35.
[95] A.I. Voloshin, N.M. Shavaleev, V.P. Kazakov, J. Lumin. 93 (2000) 115.
[96] B. Chen, N. Dong, Q. Zhang, M. Yin, J. Xu, H. Liang, H. Zhao, J. Non-Cryst. Solids 341 (2004) 53.
[97] A. Beeby, R.S. Dickins, S. Fitzgerald, L.J. Govenlock, C.L. Maupin, D. Parker, J.P. Riehl, G. Siligardi, J.A.G. Williams, Chem. Commun. (2000) 1183.
[98] R. Pizzoferrato, L. Lagonigro, T. Ziller, A. Di Carlo, R. Paolesse, F. Mandoj, D. Ricci, C. Lo Sterzo, Chem. Phys. 300 (2004) 217.
[99] R. Van Deun, P. Nockemann, Ch. Geörller-Walrand, K. Binnemans, Chem. Phys. Lett. 397 (2004) 447.

[100] J. Yu, H. Zhang, L. Fu, R. Deng, L. Zhou, H. Li, F. Liu, H. Fu, Inorg. Chem. Commun. 6 (2003) 852.
[101] F.R.G. Silava, J.F.S. Menezes, G.B. Rocha, S. Alvez, H.F. Brito, R.L. Longo, O.L. Malta, J. Alloys Compd. 303–304 (2000) 364.
[102] A. Strasser, A. Vogler, Inorg. Chem. Acta 10 (2004) 2345.
[103] Z.Q. Lao, C.S. Lee, I. Bello, S.T. Lee, Synth. Met. 111–112 (2000) 39.
[104] Z. Hong, W.L. Li, D. Zhao, C. Liang, X. Liu, J. Peng, D. Zhao, Synth. Met. 111–112 (2000) 43.
[105] V. Christou, O.V. Salata, T.Q. Ly, S. Capecchi, N.J. Bailey, A. Cowley, A.M. Chippindale, Synth. Met. 111–112 (2000) 7.
[106] X. Jiang, A.K.-Y. Jen, G.D. Phelan, D. Huang, T.M. Londer gan, L.R. Dalton, R.A. Register, Thin Solid Films 416 (2002) 212.
[107] L. Huang, K.Z. Wang, C.H. Huang, F.Y. Li, Y.Y. Huang, J. Mater. Chem. 11 (2001) 790.
[108] M.R. Robinson, M.B. O'Regan, G.C. Bazan, Chem. Commun. (2000) 1645.
[109] Y. Zheng, Y. Liang, H. Zhang, Q. Lin, G. Chuan, S. Wang, Mater. Lett. 53 (2002) 52.
[110] Z.-Q. Bian, K.-Z. Wang, Lin-Pei Jin, Polyhedron 21 (2002) 313.
[111] J. Yuan, M. Tan, G. Wang, J. Lumin. 106 (2004) 91–101.
[112] H.-G. Liu, Y.-I. Lee, S. Park, K. Jang, S. Su Kim, J. Lumin. 110 (2004) 11.
[113] H.-G. Liu, S. Park, K. Jang, X.-S. Feng, C. Kim, H.-J. Seo, Y.-I. Lee, J. Lumin. 106 (2004) 47.
[114] C. Wei Min, Y.Y. Ning, C. Dan, Mater. Chem. Phys. 80 (2003) 371.
[115] X.Z. Jiang, A.K.-Y. Jen, D. Huang, G.D. Phelan, T.M. Longergan, L.R. Dalton, Synth. Met. 125 (2002) 331.
[116] S. Capecchi, O. Renault, D.-G. Moon, M. Halim, M. Etchells, P.J. Dobson, O.V. Salata, V. Christou, Adv. Mater. 12 (2000) 1591.
[117] J. Wang, R. Wang, J. Yang, Z. Zheng, M.D. Carducci, T. Cayou, N. Peyghambarian, G.E. Jabbour, J. Am. Chem. Soc. 123 (2001) 6179.
[118] J.-C.G. Bünzli, F. Ihringer, Inorg. Chim. Acta 246 (1996) 195.
[119] Z. Hong, C. Liang, R. Li, W. Li, D. Zhao, D. Fan, D. Wang, B. Chu, F. Zhang, L.S. Hong, S.-T. Lee, Adv. Mater. 13 (2001) 1241.
[120] Q. Xu, L. Li, X. Liu, R. Xu, Chem. Mater. 14 (2002) 549.
[121] V. Tsaryuk, V. Zolin, J. Legendziewicz, Spectrochim. Acta A 54 (1998) 2247.
[122] V. Tsaryuk, J. Legendziewicz, L. Puntus, V. Zolin, J. Sokolnicki, J. Alloys Compd. 300–301 (2000) 464.
[123] V. Tsaryuk, V. Zolin, J. Legendziewicz, J. Lumin. 102–103 (2003) 744.
[124] V. Tsaryuk, V. Zolin, J. Legendziewicz, R. Szostak, J. Sokolnicki, Spectrochim. Acta A 61 (2005) 185.
[125] G. Blasse, Int. Rev. Phys. Chem. 11 (1992) 71.
[126] P. Gawryszeska, G. Oczko, J.P. Riehl, V. Tsaryuk, J. Legendziewicz, J. Alloys Compd. 380 (2004) 352.
[127] K.I. Gur'ev, M.A. Kovner, Opt. Spektr. 34 (1973) 189.
[128] Yu.V. Nefedor, V.I. Baranov, L.A. Gribov, Zh. Prikl. Spektr. 6 (1987) 246.
[129] M. Borzechowska, V. Trush, I. Turowska-Tyrk, W. Amirkhanov, J. Legendziewicz, J. Alloys Compd. 341 (2002) 98.
[130] J. Legendziewicz, O.L. Malta, M. Puchalska, V. Trush, in preparation.
[131] L. Thompson, J. Legendziewicz, J. Cybińska, Li Pan, W. Brennessel, J. Alloys Compd. 341 (2002) 312.
[132] G. Oczko, J. Legendziewicz, V. Trush, V. Amirkhanov, New J. Chem. 27 (2003) 948.
[133] F.R.G. e Silva, O.L. Malta, J. Alloys Compd. 250 (1997) 427.
[134] J. Legendziewicz, V. Amirkhanov, C. Jańczak, L. Macalik, J. Hanuza, J. Appl. Spectr. 62 (1995) 5.
[135] V. Amyrkhanov, V. Ovchynikov, J. Legendziewicz, A. Graczyk, J. Hanuza, L. Macalik, Acta Phys. Polon. 90 (2) (1996) 455.
[136] J. Sokolnicki, J. Legendziewicz, V. Amirkhanov, V. Ovchynnikov, L. Macalik, J. Hanuza, Spectrochim. Acta Part A 55 (1999) 349.
[137] J. Legendziewicz, G. Oczko, V. Amirkhanov, R. Wiglusz, V.A. Ovchynnikov, J. Alloys Compd. 300–301 (2000) 360.
[138] J. Legendziewicz, G. Oczko, R. Wiglusz, V. Amirkhanov, J. Alloys Compd. 323–324 (2001) 792.
[139] F.S. Richardson, M.F. Reid, S.S. Dallara, R.D. Smith, J. Chem. Phys. 83 (1985) 3813, and references cited therein.
[140] F.S. Richardson, J.D. Saxe, S.A. Davis, Th.R. Faulkner, Mol. Phys. 42 (1981) 1401.
[141] R. Reisfeld, J. Legendziewicz, M. Puchalska, T. Saraidarov, Opt. Mater. 26 (2004) 191.
[142] W. Stręk, J. Sokolnicki, B. Keller, M. Borzechowska, J. Legendziewicz, Proc. SPIE 3176 (1997) 259.
[143] J. Sokolnicki, K. Maruszewski, W. Strek, J. Legendziewicz, J. Sol–Gel Sci. Technol. 13 (1998) 615.
[144] W. Stręk, J. Sokolnicki, J. Legendziewicz, K. Maruszewski, R. Reisfeld, T. Pavich, Opt. Mater. 13 (1999) 41.
[145] A. Harriman, J. Photochem. 8 (1979) 205.
[146] J. Legendziewicz, W. Stręk, J. Sokolnicki, D. Hreniak, V. Zolin, Opt. Mater. 19 (2002) 175.
[147] N. Sabbatini, M. Guardigli, I. Manet, in: K.A. Gschneidner Jr., L. Eyring (Eds.), Antenna Effect in Encapsulation complexes of Lanthanide Ions, Handbook on the Physics and Chemistry of Rare Earths, Elsevier Science B.V., 1996.
[148] S. Lis, M. Elbanowski, B. Mąkowska, Z. Hnatejko, J. Photochem. Photobiol. A: Chem. 150 (2002) 233.
[149] M. Latva, H. Takalo, V.M. Mukkala, C. Matachescu, J.-C. Rodriguez-Ubis, J. Kankare, J. Lumin. 75 (1997) 149.
[150] H. Mass, A. Currao, G. Calzaferri, Angew. Chem. 114 (2002) 2607;
H. Mass, A. Currao, G. Calzaferri, Angew. Chem. Int. Ed. 41 (2002) 2495.
[151] P. Gawryszewska, L. Jerzykiewicz, M. Pietraszkiewicz, J. Legendziewicz, J.P. Riehl, Inorg. Chem. 39 (2000) 5365.
[152] P. Gawryszewska, O.L. Malta, R. Longo, F.R.G.E. Silva, K. Mierzwicki, Z. Latajka, M. Pietraszkiewicz, J. Legendziewicz, Chem. Phys. Chem. 5 (2004) 1.
[153] P. Gawryszewska, J. Sokolnicki, A. Dossing, J.P. Riehl, G. Muller, J. Legendziewicz, J. Phys. Chem. A. 109 (17) (2005) 3858.
[154] D.M. Hussey, S. Matzinger, M.D. Fayer, J. Chem. Phys. 109 (1998) 8708.
[155] J.-M. Lehn, in: V. Balzani (Ed.), Supramolecular Photochemistry, Dordrecht, Reidel, 1987, p. 29.
[156] L. Prodi, M. Maestri, V. Balzani, J.-M. Lehn, C. Roth, Chem. Phys. Lett. 180 (1991) 45.
[157] G. Mathis, C. Dumont, E.J.P. Jolu, 1990. Patent WO 92 01224.
[158] H. Autiéro, H. Bazin, G. Mathis, 2000. Patent FR/0007650.
[159] S.P. Vila-Nova, G.A.L. Pereira, R.Q. Albuquerque, G. Mathis, H. Bazin, H. Autiéro, G.F. de Sa, S. Alves Jr., J. Lumin. 109 (2004) 173.
[160] F. Bodar-Houillon, R. Heck, W. Bohnenkamp, A. Marsura, J. Lumin. 99 (2002) 335.
[161] J. Azéma, Ch. Galaup, C. Picard, P. Tisnès, P. Ramos, O. Juanes, J.C. Rodríques-Ubis, E. Burnet, Tetrahedron 56 (2000) 2673.
[162] V. Balzani, E. Berghmans, J.-M. Lehn, N. Sabbatini, R. Terőrde, R. Ziessel, Helv. Chim. Acta 73 (1990) 2083.
[163] G. Ulrich, M. Hissler, R. Ziessel, I. Manet, G. Sarti, N. Sabbatini, New J. Chem. 21 (1997) 147.
[164] R. Ziessel, L.J. Charbonnière, J. Alloys Compd. 374 (2004) 283.
[165] J. Charbonnière, R. Ziessel, M. Guardigli, A. Roda, N. Sabbatini, M. Cesario, J. Am. Chem. Soc. 123 (2001) 2436.
[166] R. Ziessel, L.J. Charbonnière, M. Cesario, T. Prange, M. Guardigli, A. Roda, A. Van Dorsselaer, H. Nierengarten, Supramol. Chem. 15 (2003) 277.
[167] N. Armaroli, V. Balzani, F. Barigelletti, M.D. Ward, J.A. McCleverty, Chem. Phys. Lett. 276 (1997) 435.
[168] Z.R. Bell, G.R. Motson, J.C. Jeffery, J.A. McCleverty, M.D. Ward, Polyhedron 20 (2001) 2045.
[169] P. Gawryszewska, M. Pietraszkiewicz, J.P. Riehl, J. Legendziewicz, J. Alloys Compd. 300–301 (2000) 283.
[170] A. Dossing, H. Toftlund, A. Hazell, J. Bourassa, P.C. Ford, J. Chem. Soc., Dalton Trans. (1997) 335.

[171] A. Dossing, M. Kristensen, H. Toftlund, J. Wolny, Acta Chem. Scand. 50 (1996) 95.
[172] A. Dossing, J. Sokolnicki, J.P. Riehl, J. Legendziewicz, J. Alloys Compd. 341 (2000) 150.
[173] E. Huskowska, I. Turowska-Tyrk, J. Legendziewicz, J.P. Riehl, New J. Chem. 26 (2002) 1461.
[174] J. Legendziewicz, E. Huskowska, O. Malta et al., in preparation.
[175] J. Sokolnicki, J. Legendziewicz, J.P. Riehl, J. Phys. Chem. B 106 (2002) 1508.
[176] E. Huskowska, P. Gawryszewska, J. Legendziewicz, Ch.L. Maupin, J.P. Riehl, J. Alloys Compd. 303–304 (2000) 325.
[177] J. Sokolnicki, J. Legendziewicz, G. Muller, J.P. Riehl, Opt. Mater. 27 (2005) 1529.
[178] F. Benetollo, G. Bombieri, A. Cassol, G. de Paoli, J. Legendziewicz, Inorg. Chim. Acta 110 (1985) 7.
[179] A. Caron, J. Guilhem, C. Riche, C. Pascard, B. Alpha, J.-M. Lehn, J.-C. Rodriguez_Ubis, Helv. Chim. Acta 68 (1985) 1577.
[180] I. Bkouche-Waksman, J. Guilhem, C. Pascard, B. Alpha, R. Deschenaux, J.-M. Lehn, Helv. Chim. Acta 74 (1991) 1163.
[181] Ch.O. Paul-Roth, J.-M. Lehn, J. Guilhem, C. Pascard, Helv. Chim. Acta 78 (1995) 1895.
[182] M. Kanesato, H. Houjou, Y. Nagawa, Kazuhisa Hiratani, Inorg. Chem. Commun. 5 (2002) 984.
[183] Xue-Lei Hu, Yi-Zhi Li, Qin-Hui Luo, Polyhedron 23 (2004) 49.
[184] O. Malta, J. Lumin. 71 (1997) 229.